

Dielectric and Energy Storage Performance of Poly(vinylidene fluoride-co-hexafluoropropylene) Thin Film with Coupling Agent

by

Zhen-Yu, Ko

A thesis submitted to the Graduate Faculty of
Auburn University
in partial fulfillment of the
requirements for the Degree of
Master of Science

Auburn, Alabama
August 8, 2020

Keywords: Permittivity, dielectric loss, breakdown strength,
energy storage density, silane additive agent

Copyright 2020 by Zhen-Yu, Ko

Approved by

Zhongyang Cheng, Chair, Professor of Material Engineering
Pengyu Chen, Assistant Professor of Materials Engineering
Siyuan Dai, Assistant Professor of Materials Engineering

Abstract

Dielectric material is an important element in the industries. It can be used for many applications, including capacitors, transistors and energy storage devices. With the development of technology, dielectrics with high permittivity, high dielectric breakdown strength and high energy storage density are required to increase the performance of electric products. In this study, a polymer-based dielectric, P(VDF-HFP), as the main dielectric material is studied for the influence of coupling/additive agent and thermal treatment on its properties. It is found that both the permittivity and electrical breakdown field can be improved by the coupling agent and thermal treatment, which is explained using the free volume theory and the microstructure.

Thermal treatment and additive agent were studied to improve the dielectric properties and energy density of P(VDF-HFP) thin film in this study. The P(VDF-HFP) thin film was fabricated by solution casting with the thickness about 12 μ m. First, different quench temperatures were applied to the film (150°C~180°C). Then, based on the result of the quench experiment, analyzing the change of the dielectric properties by adding silane as an additive agent (0.2wt% ~1.0wt%). Permittivity, dielectric loss, polarization-electric field (P-E) loop and differential scanning calorimetry (DSC) were used to analyze the sample in this study. For the thermal treatment process, it is concluded that 160°C is the best quench temperature since it results in the highest electric breakdown field and permittivity. For example, the dielectric permittivity is increased about 7% and corresponding energy density increases about 20%. Moreover, the permittivity can be further improved about 3.5% and energy density about 19% after adding silane as a coupling agent. Overall, P(VDF-HFP) thin film can improve 9% of permittivity and 42% of energy density after quenching and adding silane.

Acknowledgments

I would like to express my sincere gratitude to my advisor, Dr. Zhongyang Cheng, who helped me to develop scientific knowledge and a positive personality. With his extensive knowledge, motivation and enthusiasm, guiding me completed my graduate studies at Auburn University.

Also, I would like to give my sincere thanks to my committee member, Dr. Pengyu Chen and Dr. Siyuan Dai, for their suggestions and any kind of support for my graduate thesis and oral defense.

Moreover, I also appreciate my group member, Mr. Jindong Wei, Mr. Jiachen Liu, Ms. Liangxi Li and Mr. Weiye Wang for their help and suggestions. Special thanks to Mr. Jindong Wei, he teaches me a lot of knowledge on polymer and dielectric measurement. Overall, it is a wonderful time to work in this group.

Finally, I want to express my love and gratitude to my parents, for their encouragement and supports on my studies and also throughout my life.

Additionally, this work was partially supported by NASA through a CAN project.

Table of Contents

Abstract.....	2
Acknowledgments	3
List of Figures.....	7
Chapter 1.....	12
1.1 Dielectric Study	13
1.1.1 Capacitance	13
1.1.2 Dipole moment and Polarization	14
1.1.3 Dielectric Constant/Permittivity	17
1.1.4 Dielectric Loss	18
1.1.5 Dielectric Relaxation	20
1.2 Classification of Dielectric material	21
1.2.1 Electronic Industries Alliance Criterion	22
1.2.2 Classified by Microstructure: Polar/Non-Polar	22
1.2.3 Ferroelectric Materials.....	23
1.3 Energy Storage.....	24
1.4 Dielectric Breakdown Strength.....	27
1.4.1 Breakdown Theory.....	27
1.4.2 Microstructure Effect.....	29
(1) Polar group.....	29
(2) Molecular weight	31
(3) Polymer chain configuration.....	31

(4) Crosslinking Structure	32
(5) Crystallinity.....	33
(6) Molecular motion.....	34
(7) Additive Agent.....	35
Chapter 2.....	37
2.1 Introduction.....	37
2.2 Experimental Methodology	37
2.3 Preparation of Thin Film Sample.....	38
2.3.1 Pure P(VDF-HFP) Thin Film	38
2.3.2 P(VDF-HFP) Blend with Silane Thin Film.	39
2.4 Characterization Method.....	41
Chapter 3.....	44
3.1 Test Condition.....	44
3.2 Study of P(VDF-HFP) Thin Film	45
3.2.1 Frequency Dependency of Dielectric constant and Loss	45
3.2.2 Dielectric Breakdown Strength.....	48
3.2.3 Polarization-Electric Field Hysteresis Loops and Energy Density	50
3.2.4 Differential Scanning Calorimeter (DSC) Test.....	58
3.3 Study of P(VDF-HFP) with Silane Thin Film	61
3.3.1 Frequency Dependency of Dielectric constant and Loss.....	61
3.3.2 Dielectric Breakdown Strength.....	64
3.3.3 Polarization-Electric Field Hysteresis Loop and Energy Density	65

3.3.4 Differential Scanning Calorimeter (DSC) test.....	74
3.4 Discussion.....	78
Chapter 4.....	80
4.1 Conclusion	80
4.2 Future work.....	80
Reference	82

List of Figures

Figure 1-1 Schematic diagram for the parallel metal device	14
Figure 1-2 Schematic diagram of a single dipole	14
Figure 1-3 Schematic diagram for the dielectric material induce polarization process. The blue bar represents the electrode and grey part represents dielectrics. (a) Dielectrics without an external voltage. (b) Dipole induced by external voltage. (c) Dielectric polarization and its direction.[10-11]	15
Figure 1-4 Schematic diagram of four polarization mechanism. (a) Electronic polarization. (b) Ionic polarization. (c) Orientational polarization. (d) space charge polarization.[12].....	17
Figure 1-5 Frequency dependence of different polarization mechanisms.[12]	20
Figure 1-6 The value of $\epsilon r'$, $\epsilon r''$ and $\tan\delta$ verse frequency based on the Debye model.	21
Figure 1-7 Hysteresis loop for the ferroelectric material.	23
Figure 1-8 The energy discharge density based on the electric displacement and electric field loop. (a) linear. (b) Positive curvature. (c) Negative curvature.	25
Figure 1-9 The electric displacement verse electric field loop for four types of dielectrics [29]. The red area represents the energy density when discharging. (a) Linear dielectrics. (b) Ferroelectrics (FEs). (c) Relaxor ferroelectrics (RFEs). (d) Antiferroelectrics (AFE) [30]..	26
Figure 1-10 Dielectric strength of different polymers under different testing temperatures, including poly(methyl methacrylate), polystyrene, polypropylenes, nylon 6, poly(vinyl chloride), low-density polyethylene, polyisobutylene, polybutadiene and ethylene propylene.[35].....	30
Figure 1-11 Dielectric strength of the polyethylene with different molecular weights. [36]	31

Figure 1-12 Schematic diagram of tactic structure. (a) Isotactic. (b) Syndiotactic. (c) Atactic. [37].....	32
Figure 1-13 The dielectric strength of the polymer with different percentages of crystallinity under different testing temperatures. [39].....	34
Figure 1-14 The dielectric strength of different polymers under different testing temperatures. [41].....	35
Figure 1-15 The dielectric strength of the polymer with a different additive agent. [42]	36
Figure 2-1 Flowchart of the fabrication process.	39
Figure 2-2 Differential Scanning Calorimeter (DSC) machine.	41
Figure 2-3 Agilent 4294A impedance analyzer	42
Figure 2-4 Precision-LC100 system and H.V. Supply Amplifier.....	43
Figure 3-1 DSC of pure P(VDF-HFP) thin film.	44
Figure 3-2 Dielectric constant of pure P(VDF-HFP) thin film with different quench temperature.	46
Figure 3-3 Dielectric loss of pure P(VDF-HFP) thin film with different quench temperature. ..	46
Figure 3- 4 Dielectric constant of pure P(VDF-HFP) thin film in different quench temperature and sorted by frequency.....	47
Figure 3-5 Dielectric loss of pure P(VDF-HFP) thin film in different quench temperature and sorted by frequency.....	47
Figure 3-6 Weibull distribution plot for dielectric breakdown strength of the samples with different quench temperature.	49
Figure 3-7 Dielectric breakdown strength versus quench temperature for P(VDF-HFP).	49
Figure 3-8 P-E loop of P(VDF-HFP) thin film quench at 150°C.	50
Figure 3-9 P-E loop of P(VDF-HFP) thin film quench at 160°C.	51

Figure 3-10 P-E loop of P(VDF-HFP) thin film quench at 170°C.	51
Figure 3-11 P-E loop of P(VDF-HFP) thin film quench at 180°C.	52
Figure 3-12 P-E loop of pure P(VDF-HFP) thin film for different quench temperatures under 2000KV/cm (top) and 3000KV/cm (bottom) electric field.	53
Figure 3-13 P-E loop of pure P(VDF-HFP) thin film for different quench temperature under its maximum electric field.	54
Figure 3-14 Energy density of pure P(VDF-HFP) thin film with different quench temperatures for the charging process.	55
Figure 3-15 Energy density of pure P(VDF-HFP) thin film with different quench temperatures for the discharge process.	56
Figure 3-16 Efficiency of pure P(VDF-HFP) thin film with different quench temperature.	56
Figure 3-17 Energy density of pure P(VDF-HFP) thin film with different quench temperatures for the charging process under different electric fields.	57
Figure 3-18 Energy density of pure P(VDF-HFP) thin film with different quench temperatures for the discharge process under different electric fields.	57
Figure 3-19 Efficiency of pure P(VDF-HFP) thin film with different quench temperature under different electric fields.	58
Figure 3-20 The heating process of DSC for pure P(VDF-HFP) thin film quench at different temperatures.	59
Figure 3-21 The cooling process of DSC for pure P(VDF-HFP) thin film quench at different temperatures.	60
Figure 3-22 Enthalpy of the P(VDF-HFP) thin film with different quench temperature calculated by the DSC result.	60

Figure 3-23 Dielectric constant of P(VDF-HFP) thin film with different concentrations of silane.	62
Figure 3-24 Dielectric loss of P(VDF-HFP) thin film with different concentrations of silane. ..	62
Figure 3- 25 Dielectric constant of P(VDF-HFP) thin film with different concentrations of silane and sorted by frequency.	63
Figure 3-26 Dielectric loss of P(VDF-HFP) thin film with different concentrations of silane and sorted by frequency.	63
Figure 3-27 Weibull distribution plot for dielectric breakdown strength of the samples with different concentrations of silane.	64
Figure 3-28 Dielectric breakdown strength of P(VDF-HFP) thin film with different concentrations of silane.	65
Figure 3-29 P-E loop of P(VDF-HFP) thin film with 0.2wt% of silane.	66
Figure 3-30 P-E loop of P(VDF-HFP) thin film with 0.4wt% of silane.	66
Figure 3-31 P-E loop of P(VDF-HFP) thin film with 0.6wt% of silane.	67
Figure 3-32 P-E loop of P(VDF-HFP) thin film with 0.8wt% of silane.	67
Figure 3-33 P-E loop of P(VDF-HFP) thin film with 1.0wt% of silane.	68
Figure 3-34 P-E loop of P(VDF-HFP) thin film with different concentrations of silane under 2000 KV/cm (top) and 3000KV/cm (bottom) electric field.	69
Figure 3-35 P-E loop of P(VDF-HFP) thin film with different concentrations of silane under its maximum electric field.	70
Figure 3-36 Energy density of P(VDF-HFP) thin film with different concentrations of silane for the charging process.	71
Figure 3-37 Energy density of P(VDF-HFP) thin film with different concentrations of silane for discharging process.	72

Figure 3-38 Efficiency of P(VDF-HFP) thin film with different concentrations of silane.....	72
Figure 3-39 Energy density of P(VDF-HFP) thin film with different concentrations of silane for the charging process under different electric fields.	73
Figure 3-40 Energy density of P(VDF-HFP) thin film with different concentrations of silane for the discharging process under different electric fields.	73
Figure 3-41 Efficiency of P(VDF-HFP) thin film with different concentrations of silane under different electric fields.	74
Figure 3-42 The heating process of DSC for P(VDF-HFP) thin film with different concentrations of silane.	75
Figure 3-43 The cooling process of DSC for P(VDF-HFP) thin film with different concentrations of silane.	76
Figure 3-44 Enthalpy of P(VDF-HFP) thin film with different concentrations of silane calculated by DSC result.....	76
Figure 3-45 Enthalpy and the peak temperature of P(VDF-HFP) thin film with different concentrations of silane at the endothermic peak (~49°C) calculated by DSC result.	77
Figure 3-46 Enthalpy and the peak temperature of P(VDF-HFP) thin film with different concentrations of silane at the endothermic peak (~133°C) calculated by DSC result.	77
Figure 3-47 Enthalpy and the peak temperature of P(VDF-HFP) thin film with different concentrations of silane at the endothermic peak (~162°C) calculated by DSC result.	78

Chapter 1

Introduction

The main objective of this study is to determine the influence of thermal treatment and coupling/additive agent on the dielectric properties and energy density performance of P(VDF-HFP). The dielectric materials can be utilized to fabricate various devices, such as capacitors and energy storage devices, for different applications, such as the mobile electronic device, hybrid electric vehicles and electrical pulse device [1]. For the applications mentioned above, the performance of a device or a dielectric is evaluated by many parameters/properties including dielectric permittivity, loss, electric breakdown field, energy density, density [2]. Besides these, flexibility and eco-friendly are also important characteristics for the dielectrics [3-5]. Thus, the polymer-based dielectric material, P(VDF-HFP), is selected for this study. For example, P(VDF-HFP) exhibited a low dielectric loss, low density and high breakdown field and excellent flexibility, which are favorable for the development of high-performance energy storage devices [6-7]. Plus, from the manufacturing process perspective, P(VDF-HFP) is easy to be processed/fabricated into a thin film.

Moreover, microstructure modification can be an alternative and effective method to improve the dielectric property and further strengthen its performance. Recently, adding ceramic composite is a popular method to enhance the dielectric performance of polymer-based dielectric materials. Although the ceramic composite has very higher permittivity, the breakdown strength is much weaker than polymer, which can be a significant limitation. Additionally, it is very difficult to achieve the uniform distribution of ceramic composite when fabricating the thin film, especially when the thickness of the thin film is very small. Then, the issue can be addressed by using coupling agent alternatively due to the size and properties of coupling agent. Therefore, in this study, it showed improvement of the dielectric properties when adding coupling agent. Silane is

the coupling agent used in this study. It was believed that the silane can be served as a small molecular to fill up the space between the polymer chains and also strengthen the interaction among polymer chains providing an additional improvement on the electric breakdown field [8].

1.1 Dielectric Study

Dielectric property is a very important property for material using in the electrical industries. In this part, it would introduce the main principle of the dielectric property, which included the factors that influence the permittivity, dielectric loss, energy density and its applications. By understanding the basic knowledge of dielectric property, it will easy to improve the dielectric performance of our research samples.

1.1.1 Capacitance

Capacitance describes the ability that a capacitor can store the electrical charge. The concept of capacitance can be further explained by the parallel metal plate experiment, demonstrated in **Figure1-1**. For the parallel metal plate, applying voltage V into the parallel metal plate with the distance between two plates L. Then, measured the amount of charge (q) that accumulate on the surface of the plates. Based on the concept, the capacitance can be calculated by the formula as below:

$$C = \frac{q}{V} \quad (1.1)$$

However, the capacitance can also be described as below:

$$C = \epsilon \epsilon_0 \frac{A}{L} \quad (1.2)$$

where A is the plate area, L is the distance between two parallel plates, ϵ_0 is the dielectric constant for the free space (8.85×10^{-12} F/m) [9] and the ϵ is the dielectric constant/permittivity of

the dielectric material. By equation (1.2), it can be known that the ability of electrical storage increases with increasing permittivity.

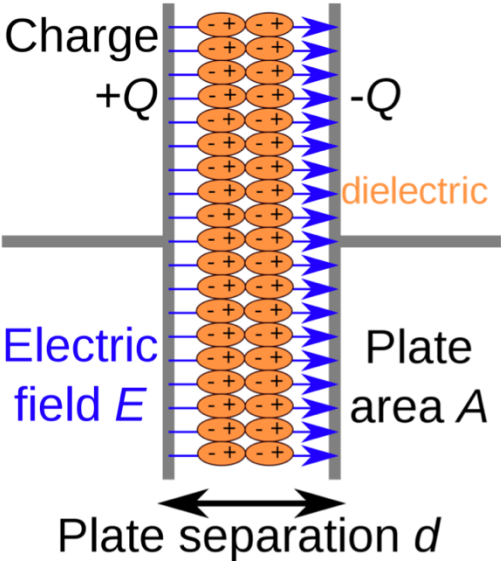


Figure 1-1 Schematic diagram for the parallel metal device

1.1.2 Dipole moment and Polarization

This section explains the permittivity of material and the fundamental knowledge of it. First, the concept of an electric dipole is very important to help us realized the fundamentals, which shown in **Figure 1-2**.

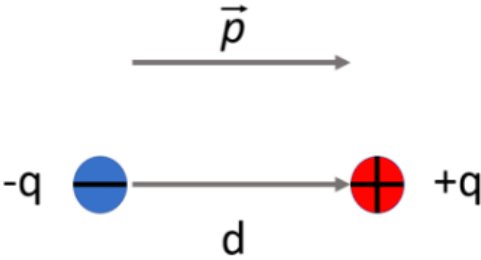


Figure 1-2 Schematic diagram of a single dipole

As showed in **Figure 1-2**, charges can be separated into two same amount of charge but opposite sign under the external electric field. The distance between two separated electric charge is d and generate dipole moment (\vec{p}), which with the direction from negative to positive. Then, the amplitude of the dipole moment can be described by the formula as following:

$$p = qd \quad (1.3)$$

Then, when considering the entire system, a specific value can be calculated to represent the overall dipole moment (\vec{p}) in one unit volume, which is the polarization (\vec{P}). The formula that described the relation of \vec{P} and \vec{p} shown as below:

$$\vec{P} = \frac{d\vec{p}}{dv} \quad (1.4)$$

where v is the volume.

When compared the difference of dipole moment and polarization, the unit of those two was worth to discuss. For the dipole moment, $p = qd$, with the unit in coulomb·meter (C·m). And for the polarization, $\vec{P} = \frac{d\vec{p}}{dv}$, with the unit in coulomb/meter² (C/m²). Therefore, polarization can express how the charge accumulated on the surface of the dielectric material.

To further understand the mechanism of the polarization, **Figure 1-3** showed the relationship between the single dipole moment and the overall system. Then, combining the knowledge from the capacitance; the polarization exerts a huge impact on the dielectric constant.

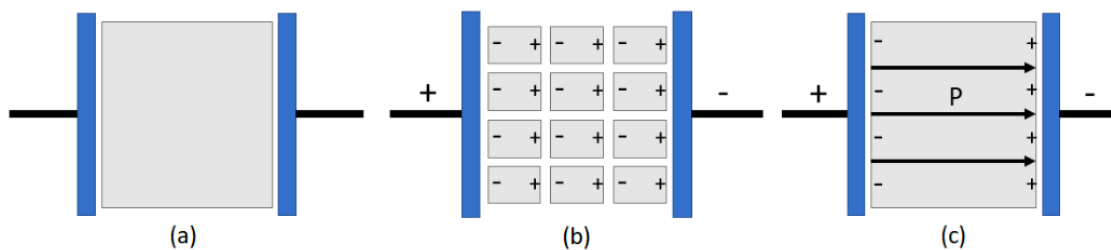


Figure 1-3 Schematic diagram for the dielectric material induce polarization process. The blue bar represents the electrode and grey part represents dielectrics. (a) Dielectrics without an

external voltage. (b) Dipole induced by external voltage. (c) Dielectric polarization and its direction.[10-11]

Normally, four common polarization mechanisms contained electronic polarization (shown as **Figure1-4**), ionic polarization, orientational polarization and space charge polarization [12,13]. For the electronic polarization, it generated by the outer electron cloud displace from the inner positive nucleus under the external electric field. In addition, electronic polarization is independent of temperature. For the ionic polarization, it generated by ionic displacement when applied external electric field. This response very weakly depends on the temperature. For orientational polarization, it caused by the aligned dipole along with the external electric direction and depends on the temperature strongly. For the space charge polarization, caused by the separation of the positive and negative charges. This mechanism depends on temperature. The mechanism of the polarization would result in a different characteristic response. The difference between them would be further discussed in the next section.

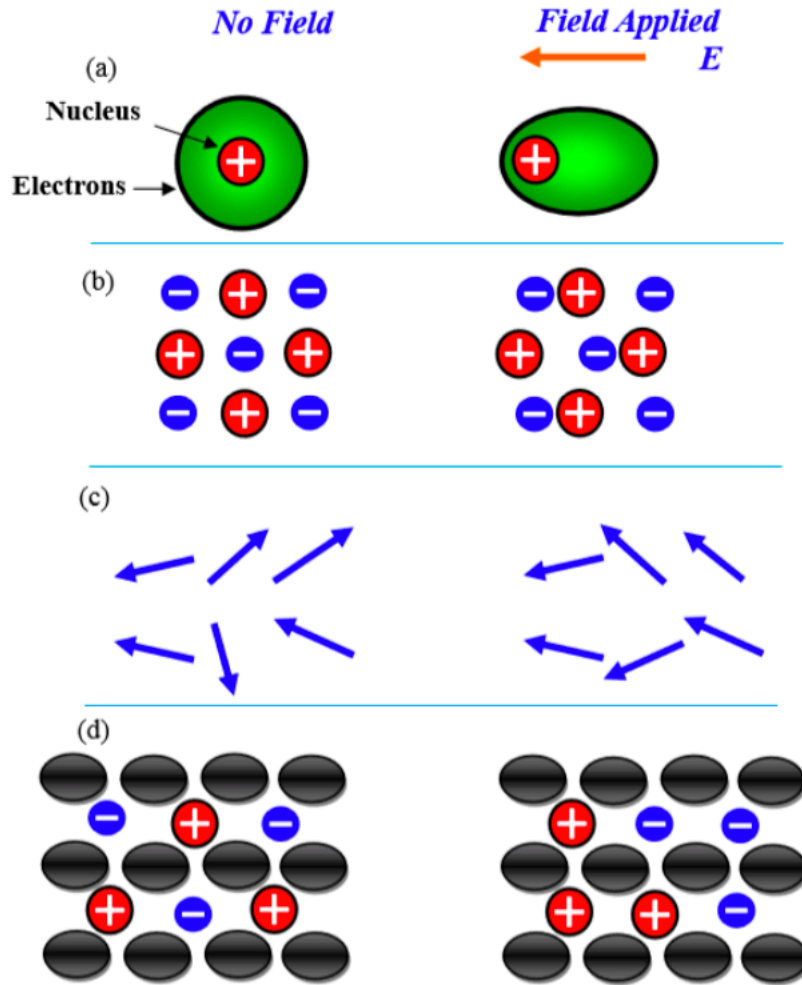


Figure 1-4 Schematic diagram of four polarization mechanism. (a) Electronic polarization. (b) Ionic polarization. (c) Orientational polarization. (d) space charge polarization.[12]

1.1.3 Dielectric Constant/Permittivity

For a dielectric material, it exhibited polarization when subject to an external electric field. This phenomenon is based on the microstructure of the atoms, which has explained from the last section. To further understanding the concept, the relationship should be defined by the formula, which can be expressed by the following equation [14]:

$$\vec{D} = \varepsilon_0 \vec{E} + \vec{P} \quad (1.5)$$

where \vec{D} is electric displacement, ε_0 is the dielectric constant in a vacuum (8.85×10^{-12} F/m) and \vec{P} is polarization. Then, equation (1.5) can also be expressed as:

$$\vec{D} = \varepsilon \vec{E} = \varepsilon_0 \varepsilon_r \vec{E} \quad (1.6)$$

where ε_r is the relative dielectric constant/permittivity, ε is the dielectric constant/permittivity of the dielectric material.

Then, based on the equation (1.5) and (1.6), the relationship between polarization and external DC electric field can be expressed as:

$$\vec{P} = (\varepsilon_r - 1)\varepsilon_0 \vec{E} = \chi \varepsilon_0 \vec{E} \quad (1.7)$$

where $\chi = \varepsilon_r - 1$, defined as susceptibility of the material.

However, previous discussions and equations are based on the DC electric field; the material would demonstrate a different dielectric property in the AC conditions. In other words, dielectric materials are very sensitive to the frequency. That means dielectric material would change its property when applying electric field vary in frequency. Therefore, the formula should be modified; electric displacement, polarization and dielectric constant become a complex number. The formula can be defined as:

$$\vec{D}^* = \varepsilon_0 \vec{E} + \vec{P}^* \quad (1.8)$$

$$\vec{P}^* = (\varepsilon_r^* - 1)\varepsilon_0 \vec{E} \quad (1.9)$$

1.1.4 Dielectric Loss

As we know from the last section, dielectric property strongly depends on the frequency applied to the material. Dielectric loss came from the inherent dissipation of electromagnetic energy. When dielectric material under an AC field, the dielectric constant/permittivity at each frequency is complex and can be expressed as:

$$\varepsilon_r^* = \varepsilon_r' - j\varepsilon_r'' \quad (1.10)$$

where ε_r' is the real part of the permittivity, ε_r'' is the imaginary part of the permittivity and j is a constant depends on materials, and both ε_r' and ε_r'' are dependent on frequency. In dielectric material, ε_r' represent the energy stored in the medium and ε_r'' is the energy converted to heat. The dielectric loss ($\tan\delta$) of dielectric material is defined as the ratio of ε_r'' to ε_r' , which can be expressed as:

$$\tan\delta = \frac{\varepsilon_r''}{\varepsilon_r'} \quad (1.11)$$

It has to be mentioned that for a dielectric polarization, there is a relation between the real and imaginary part. That is, Kramers-Krong relations [15]:

$$\varepsilon_r'(w) = \varepsilon_{r\infty} + \frac{2}{\pi} \int_0^\infty \frac{u\varepsilon_r''(u)}{u^2-w^2} du \quad (1.12)$$

$$\varepsilon_r''(w) = \frac{2}{\pi} \int_0^\infty [\varepsilon_r'(u) - \varepsilon_{r\infty}] \frac{w}{u^2-w^2} du \quad (1.13)$$

where w is the angular frequency, $\varepsilon_{r\infty}$ is the dielectric constant at the high-frequency limit.

The Kramers-Krong relationship is also illustrated in **Figure 1-5**.

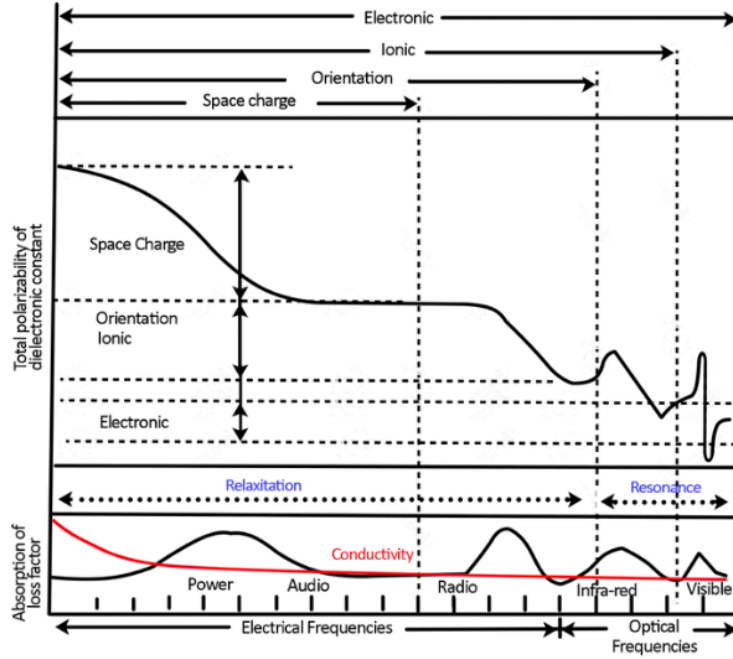


Figure 1-5 Frequency dependence of different polarization mechanisms.[12]

1.1.5 Dielectric Relaxation

In general, relaxation defines as a response that after the external stimulation was removed. The response of the relaxation is a time-dependent process. The relaxation can be influenced by lots of factors, including the material, chemical composition, temperature condition. The assumption based on the Debye model is the popular one on describing dielectric relaxation. In the Debye equation, it assumed the material in the ideal condition, meaning no interaction between the dipoles. The Debye equation is [16]:

$$\epsilon_r' = \epsilon_{r\infty} + \frac{\epsilon_{rs} - \epsilon_{r\infty}}{1 + \omega^2 \tau_0^2} \quad (1.14)$$

$$\epsilon_r'' = \frac{(\epsilon_{rs} - \epsilon_{r\infty}) \omega \tau_0}{1 + \omega^2 \tau_0^2} \quad (1.15)$$

$$\tan \delta = \frac{\epsilon_r''}{\epsilon_r'} = \frac{(\epsilon_{rs} - \epsilon_{r\infty}) \omega \tau_0}{\epsilon_{rs} + \epsilon_{r\infty} + \omega^2 \tau_0^2} \quad (1.16)$$

where ϵ_{rs} is static permittivity, $\epsilon_{r\infty}$ is the permittivity at the high-frequency limit, ω is the angular frequency and τ_0 is characteristic relaxation time.

Then, based on the Debye model, the ideal condition, the relationship between those three parameters can be expressed by **Figure 1-6**.

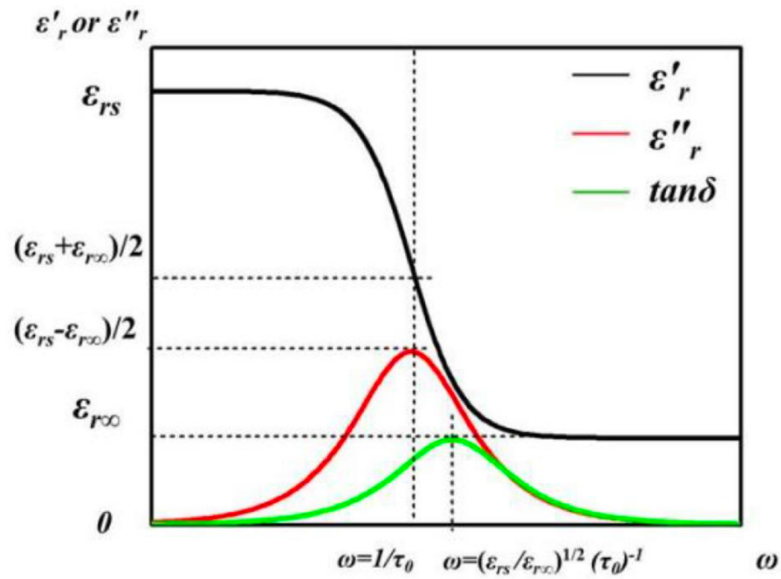


Figure 1-6 The value of ϵ'_r , ϵ''_r and $\tan\delta$ verse frequency based on the Debye model.

1.2 Classification of Dielectric material

Dielectric material has lots of applications. Then, it can be sorted into some small group by their mechanism. The performance of loss, permittivity, relaxation time, breakdown field and energy density are the main properties for organizing the group. Understanding the categories of the dielectric materials is a very important work before doing the research. In this section, it will introduce some popular dielectric material categories.

1.2.1 Electronic Industries Alliance Criterion

Electronic Industries Alliance (EIA) sorts the dielectric material into three main categories depends on its dielectric properties [17]. This method is good for industrial applications. For type I, the dielectric material with lower permittivity between 15-500 and the loss is less than 0.003. Besides, the working temperature is from -55 °C and 85 °C. Type II contains the dielectric material with permittivity between 500 to 2000. Type III is the dielectric material with very high capacitance and low dielectric breakdown strength. Therefore, industries can find the appropriate dielectric material depends on their applications.

1.2.2 Classified by Microstructure: Polar/Non-Polar

Moreover, dielectric materials can also be sorted by their microstructure: non-polar and polar [18]. The main difference between the polar and nonpolar materials is whether they possessed permanent dipole moments. Based on the knowledge we discussed above, the permanent dipole moment can significantly influence the polarization process [19]. Then, polarization is the main factor related to the permittivity. Usually, the nonpolar materials have lower permittivity than the polar material. Take some inorganic material for instance. The permittivity of silicon ≈ 3.7 , carbon ≈ 2.0 , quartz ≈ 4.4 and paraffin $\approx 2.0\sim 2.5$. Then, the application of nonpolar dielectric material is limited. On the other hand, polar materials have an asymmetric structure, which exhibited a permanent dipole moment without applying any external electric field. This is due to the dipoles originally align in a similar direction. This material also named as pyroelectric material. And the polarization caused by the dipole moment without an external electric field called spontaneous polarization. Moreover, the spontaneous polarization can change its direction along with the direction of the external electric field; this material called ferroelectric materials.

1.2.3 Ferroelectric Materials

Ferroelectric materials exhibited very unique dielectric properties, which allow it equipped with very high dielectric constant [20,21]. Therefore, ferroelectric materials are a very important field for our research. By observing the P-E loop of the ferroelectric materials, it showed hysteresis behavior. As shown in **Figure 1-7**, the ferroelectric materials remained a certain value of polarization after removing the external electric field which called remanent polarization. And it needs to apply a reverse electric field to offset the polarization; this electric field was called coercive field.

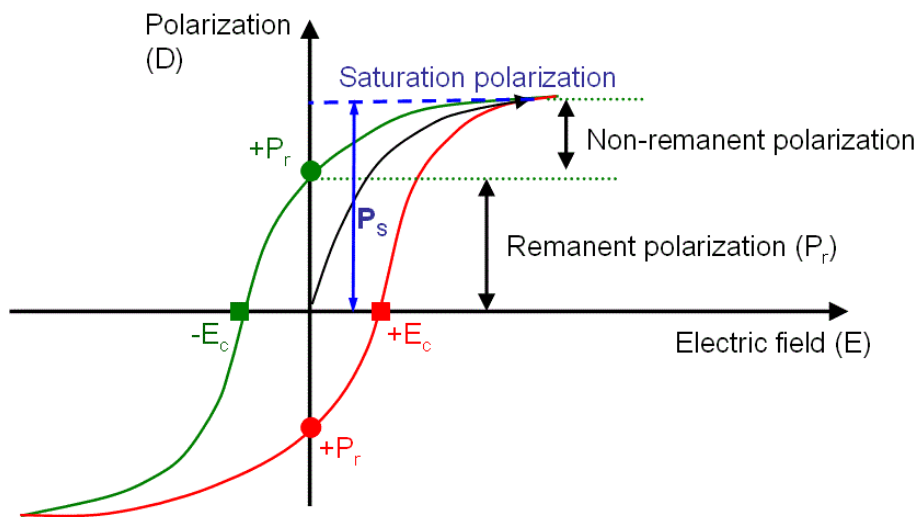


Figure 1-7 Hysteresis loop for the ferroelectric material.

Despite the ferroelectric materials have a very high dielectric constant, it is very sensitive to the temperature, especially when the temperature close to the phase transition temperature. It existed a critical temperature where the dielectric constant can change significantly called Curie Temperature [22], which defined the phase transition from the ferroelectric to paraelectric. The reason for that is due to the symmetric units increase with increasing temperature, which makes the paraelectric phase a non-polar dielectric. Therefore, the dielectric behavior of these two phases is completely different. For the paraelectric phase, the dielectric constant is dependent on temperature by the Curie-Weiss laws [22]:

$$\varepsilon_r' = \frac{C}{T-T_c} \quad (1.17)$$

where C is Curie constant and T_c is the Curie temperature.

1.3 Energy Storage

Energy storage density determines the ability that a dielectric material can store electric energy when subject to an external electric field. Based on this mechanism, dielectric materials can be used as capacitors in the electronic device to stabilize the power supply. Meanwhile, the dielectric loss determined how much energy loss during the discharging process, which is converted into heat. Energy storage density can be calculated by formula as following [23,24]:

$$U = \int_0^D \vec{E} \cdot d\vec{D} \quad (1.18)$$

where U is the energy storage density, \vec{E} is the electric field applied on the dielectric material and \vec{D} is the electric displacement. Then, if combined the equation (1.18) and equation (1.6), the equation can be expressed as [25]:

$$U = \frac{1}{2} \varepsilon_r' \varepsilon_0 \vec{E}^2 \quad (1.19)$$

Equation (1.19) is for linear dielectrics, it can be easier to understand the factors that influence the ability of energy density, which can be determined by the permittivity and the electric field. Therefore, increasing the permittivity is an important task to improve the energy density of the dielectric material.

Then, when considering the equation (1.18), the energy storage can be defined as the blue area on **Figure 1-8**, where three different types of D~E (P-E) relationships are presented. It can be found that the relationship between displacement and the electric field is also critical.

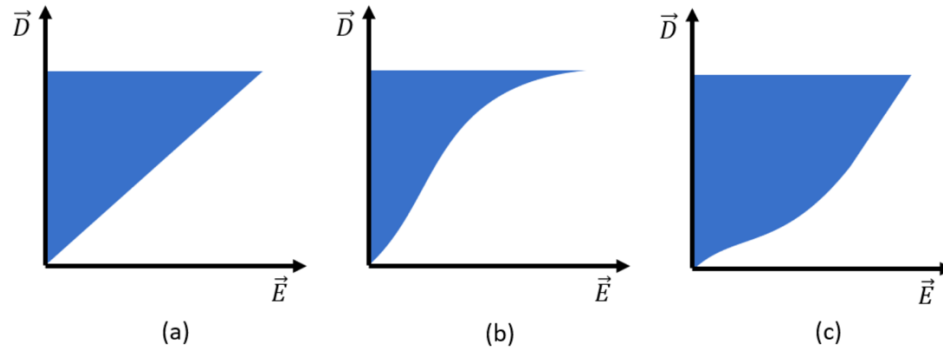


Figure 1-8 The energy discharge density based on the electric displacement and electric field loop. (a) linear. (b) Positive curvature. (c) Negative curvature.

As discussed above, improving the permittivity of dielectric materials can increase the energy storage density which is beneficial to our research. However, in the equation (1.18), it can be found that the electric field also plays an important role. Usually, the material has a limit value of the applied electric field, which can be defined as E_{max} . The details of the E_{max} will be further explained in the next section. In general, when the applied electric field above E_{max} , the dielectric material may breakdown and cannot be used anymore. Therefore, in order to increase the energy density of a dielectric material, it needs to strengthen both the permittivity and E_{max} (also defined as dielectric breakdown strength E_b).

However, most of the dielectric materials do not have high permittivity and E_b at the same time. Usually, inorganic material has a relatively high dielectric than organic material but a lower E_b [26], but organic dielectrics such as polymers exhibit a high E_b but a lower permittivity. Therefore, it is interesting to combine the advantage of both organic and inorganic materials into one material – composite in order to get better energy storage density material.

In general, there are four common types of dielectrics, as shown in **Figure 1-9**. As the concept mentioned above, the area between the curve and the y-axis is the energy stored by the dielectrics. Therefore, it can be noticed that the remnant polarization can also influence the amount

of the energy stored in dielectrics. For the linear dielectric, shown in **Figure 1-9(a)**, this kind of dielectric usually has high dielectric strength and low dielectric loss; however, it would not be a good dielectric material for energy storage due to their relative low permittivity. Then, the performance of the linear dielectrics is limited. Second, ferroelectric, shown in **Figure 1-9(b)**, which usually exhibited a high permittivity. However, it cannot store large amounts of energy due to the large hysteresis [27,28]. Then, for the relaxor ferroelectrics and antiferroelectrics, shown in **Figure 1-9(c,d)**, exhibiting better ability of energy storage because the remnant polarization of these two dielectrics is very small.

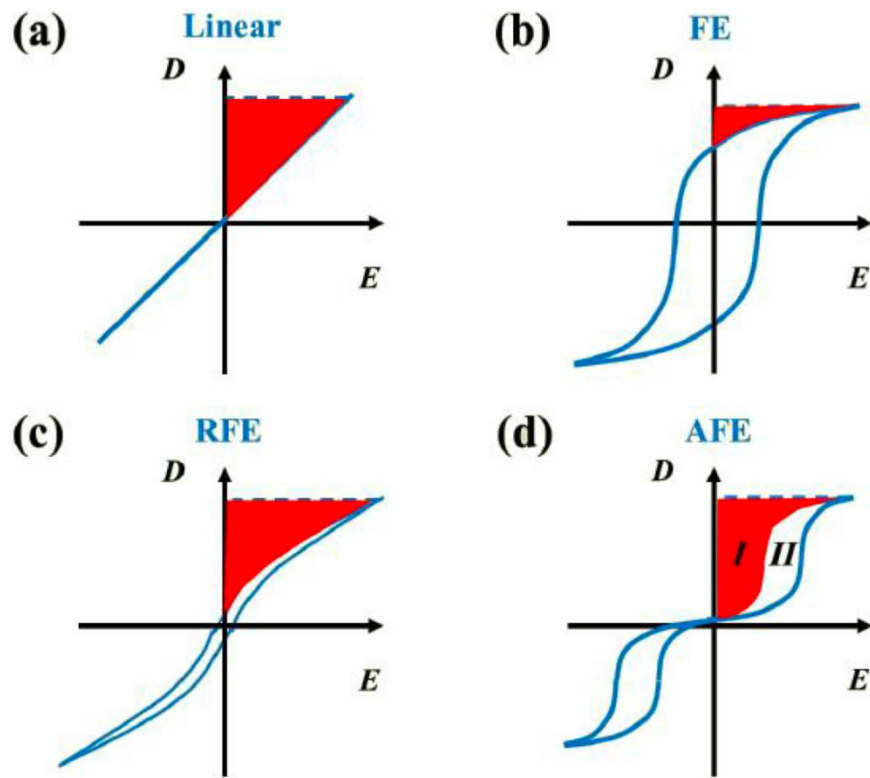


Figure 1-9 The electric displacement versus electric field loop for four types of dielectrics [29]. The red area represents the energy density when discharging. (a) Linear dielectrics. (b) Ferroelectrics (FEs). (c) Relaxor ferroelectrics (RFEs). (d) Antiferroelectrics (AFEs) [30].

1.4 Dielectric Breakdown Strength

Dielectric breakdown strength is a critical point that transferred the dielectric material from insulative to conductive. It is an irreversible process. The dielectrics would be damaged when the overload of the external electric field; therefore, when the applied electric field above the breakdown strength, the energy stored in the dielectrics would be released immediately. The breakdown strength can be defined as:

$$E_b = \frac{V_b}{d} \quad (1.20)$$

where the E_b is the breakdown strength, V_b is the maximum voltage can be applied on the dielectrics and d is the thickness of the dielectrics. These parameters reflected the parallel plate experiment condition.

1.4.1 Breakdown Theory

In order to realize the mechanism behind the breakdown phenomenon, it needs to consider the microstructure of the dielectrics and the relationship between the dielectrics and electrons. In addition, the breakdown strength is also influenced by the testing temperature and moisture. In this section, it will introduce some effects that may influence the dielectric breakdown strength.

Thermal breakdown is a common concept when analyzing polymer-based dielectrics. Heat would be generated when the dielectrics under the electric field. As mentioned above, the amount of heat would be generally determined by the dielectric loss. Therefore, the dielectric material would become hot under the external electric field. Plus, the dielectrics would increase its conductivity when it is at the high temperature. As a result, the heat would be generated quickly as the temperature increased. In this situation, if the heat generation overpassed the heat dispersion, the temperature would high enough to make the dielectrics decomposition or carbonation. Finally, the dielectrics breakdown and cannot store any electric energy. [31]

Moreover, electric breakdown can be caused by another mechanism, which caused by collision ionization. Under the electric field, the high speed electric result in the huge electric current [32]. This huge current can also make dielectrics breakdown. That explained the electronic process could be an important factor to influence our result. In addition, physical and chemical degradation may happen under the electric field, too. It would change the dielectric property of the dielectrics and further influence the dielectric strength. This phenomenon usually happened when the dielectrics under the long-term external electric field. However, the mechanism discussed above was based on the impact of the electric field.

Space charge can also influence the dielectric strength. As we know, space charge could distort the electric field in the dielectrics; it can either enhance or weaken the local electric fields [33]. It can be concluded that the Maxwell stress was enhanced when enhancing the local electric field by the space charge, which can generate cracks easily. That is due to the extra charge can also be accelerated by the electric field and then release the energy in the medium. Therefore, the enhanced part of the dielectric break easily [34].

Moreover, the thickness of the thin film also exerts a significant influence on the breakdown strength. In general, the dielectric breakdown strength increase with increasing thickness. For the relatively thinner film, the trapped charge can flow easily rather than gathering together. Therefore, it can withstand a higher electric field. Plus, thinner films have more grain boundary density due to the small size of grains, which can also enhance the dielectric breakdown strength. Therefore, based on the concept above, the thickness can be a very important parameter in this study. The relationship between thickness and dielectric breakdown strength can be expressed by the formula below:

$$E_b = kd^{-n} \quad (1.21)$$

where E_b is dielectric breakdown strength, k is dependent on material and n is power index. According to the data showed by Forlani and Minnaja, n is around 0.5 for thinner thickness and 0.25 for thicker thickness. The formula was based on empirical results. Therefore, it may have a different result for our study.

1.4.2 Microstructure Effect

In this section, it will introduce some factors which can influence the dielectric strength directly. As mentioned previously, the mechanism that influences the breakdown field is a complicated issue. It is more likely a combination factor, including thermal breakdown, electric breakdown, long-term breakdown and space charge. It probably has some complicated mechanism that we didn't mention; it can be sure that the breakdown process is very complex. Therefore, in this section, it will discuss the details of the factors that can influence the dielectric strength significantly and it can be further modified in order to enhance the performance of our dielectrics.

(1) Polar group

From **Figure 1-10**, indicating the dielectric strength would significantly decrease at a certain point for some polymers, which can be defined as a critical point. The temperature at the point is called critical temperature (T_c). However, not all of the dielectric in **Figure 1-10** exhibits this phenomenon. This is dependent on the structure of the polymer: polar or not. For the nonpolar dielectrics, it has an obvious critical temperature (T_c). For polar dielectrics, it doesn't have an obvious critical temperature. The main reason is the dipole created by the polar group. During the low temperature and below the critical temperature, the mechanism of the breakdown process was

determined by the electron process. The dipole would interrupt or slow down the energy transmit, which can fortify the dielectric strength.

However, when raising the temperature above the critical temperature (T_c), the polarization generated by the dipole becomes weak. Plus, the mechanism of the breakdown would be dominated by the thermal and electromechanical breakdown. Therefore, for the high temperature region, it was a relatively complicated process. It didn't exhibit a clear impact on the dielectric strength.

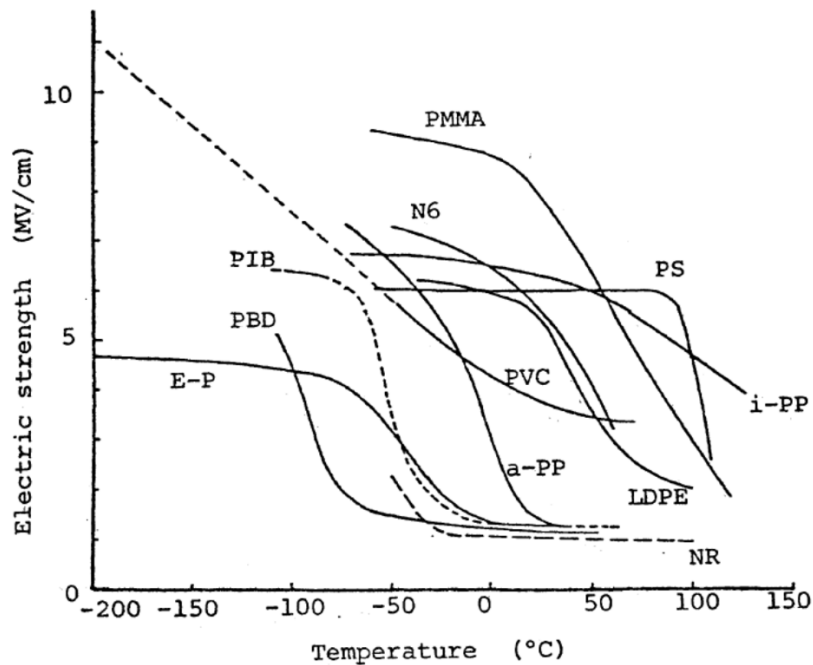


Figure 1-10 Dielectric strength of different polymers under different testing temperatures, including poly(methyl methacrylate), polystyrene, polypropylenes, nylon 6, poly(vinyl chloride), low-density polyethylene, polyisobutylene, polybutadiene and ethylene propylene.[35]

(2) Molecular weight

For **Figure 1-11** it showed that the molecular weight affects the dielectric strength. Usually, the dielectric strength would increase with increasing molecular weight. However, it is more precise to say that the polymer with higher molecular weight would have more probability to be equipped with better electric strength because it may exist another factor influence the dielectric properties of the polymer when modifying the molecular weight of the polymer.

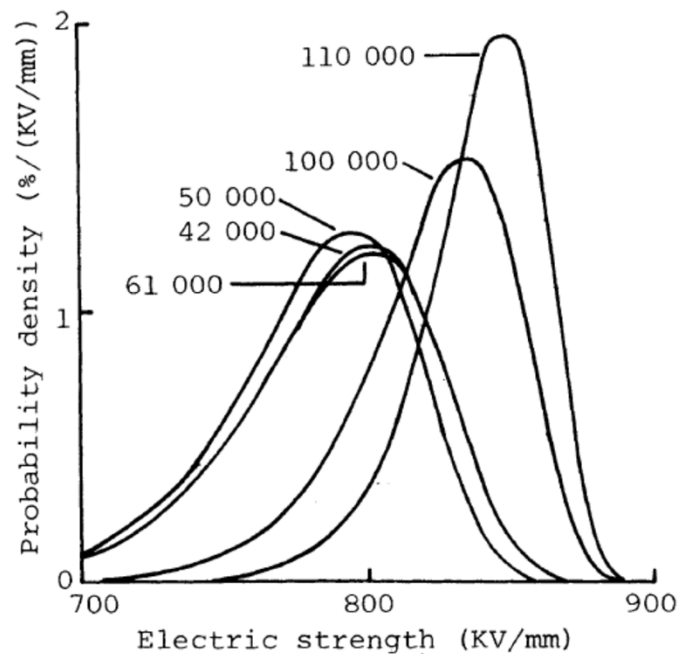


Figure 1-11 Dielectric strength of the polyethylene with different molecular weights.

[36]

(3) Polymer chain configuration

The tacticity of polymer will affect the dielectric breakdown strength. From **Figure 1-10**, polypropylenes have higher dielectric strength in the lower temperature; however, the dielectric strength significantly decreases with increasing the temperature. This is mainly due to the configuration of the polymer. For the low temperature, the polypropylenes have an atactic structure

in which the substituents were randomly placed along the main chain. On the other hand, the substituents would move to one side and form an isotactic structure. The electric strength would decrease when increasing temperature because the electrons would be interrupted by the irregular structure during the low temperature region [37]. **Figure 1-12** showed a schematic diagram of the different tactic structures.

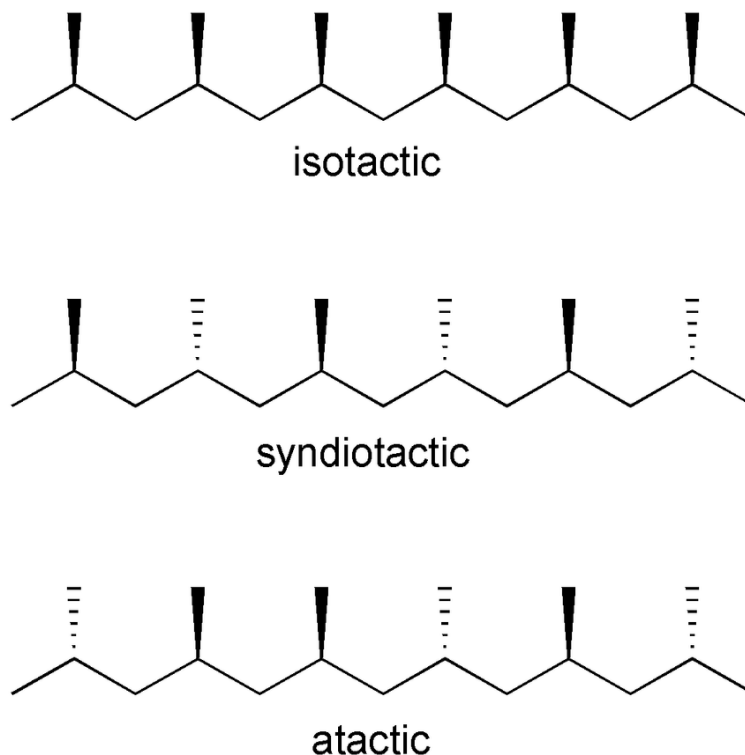


Figure 1-12 Schematic diagram of tactic structure. (a) Isotactic. (b) Syndiotactic. (c) Atactic. [37]

(4) Crosslinking Structure

Crosslink is the bond that connects between the polymer chains; it can be either covalent bonds or ionic bonds. The polymer will increase the viscosity when it contains more crosslinks between chains. This is due to the free volume between polymer chains was filled by the bonds [38]. Therefore, the electrons have more probability to be interrupted when applied external

electric field, which results in the higher dielectric strength. Overall, it can say that the dielectric strength would increase by increasing the crosslink density.

(5) Crystallinity

In general, the crystalline polymer can be sort into two main phases/regions: crystalline and amorphous. The main difference between the two phases is the organization of the structure. The crystalline structure is ordered and usually equipped with better mechanical strength and rigidity; however, amorphous structure is more flexible and elastic because the chains were not fixed. Therefore, dielectric strength can be different in two different phases. Crystallinity defined the percentage of crystalline structure in the polymer. **Figure 1-13** showed the relationship between the crystallinity and the electric strength of polyethylene. It can be found that the electric strength decrease with increasing the degree of crystallinity when it under 80°C. However, when the temperature above 80°C, the result is different. This is due to the depth of the shallow trap increase when decreasing the crystallinity, which allowing to interrupt more electrons when applied voltage. On the other hand, when the temperature higher than 80°C, the electromechanical breakdown mechanism dominated the breakdown process. Therefore, the polymer with higher crystallinity can bear more voltage due to better mechanical strength of the crystalline structure.

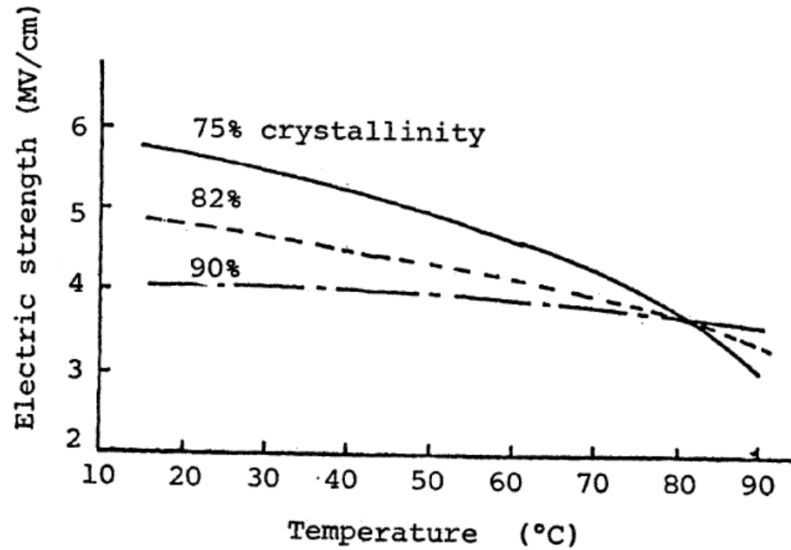


Figure 1-13 The dielectric strength of the polymer with different percentages of crystallinity under different testing temperatures. [39]

(6) Molecular motion

As we know, polymer consisted of polymer chains. The polymer cannot occupy all the space; it exists some free volume between chains. The free volume between chains influences the viscosity of the polymer and its properties. This concept was first introduced by Fox and Flory in 1950 [40]. The free volume increases with increasing temperature; it will make polymer chains have more space to move, meaning increase the ability of molecular motion. During the heating process, the polymer would change from the glass-like phase to the rubber-like phase; this process allowed the polymer to have some mobility. Besides that, molecular motion can influence the dielectric strength of polymers. From **Figure 1-14**, it can be found that the polymers have lower dielectric strength when it reached the glass transition temperature. This phenomenon verified the free volume theory related to the dielectric strength during the electrons passing process.

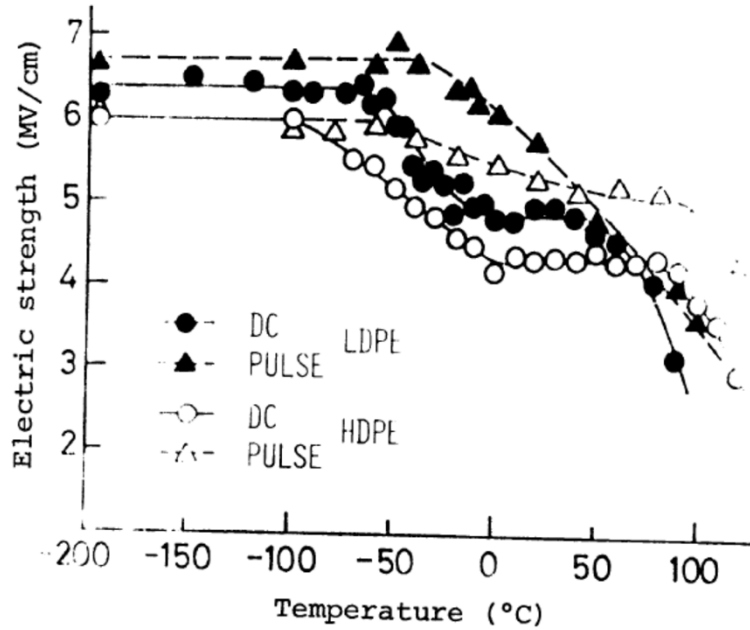


Figure 1-14 The dielectric strength of different polymers under different testing temperatures. [41]

(7) Additive Agent

Additive agent can change the dielectric property of the polymers; it can either increase or decrease the dielectric strength which depended on the property of additive agent [42]. From **Figure 1-15**, it can verify that different additive agents can result in a different result. The difference between the two additive agents is conductivity. AS-1 is conductive and provided extra charge to the polymer. Based on this phenomenon, AS-1 would increase the conductivity and reduce the dielectric strength of the polymer. On the other hand, Pyrene has the opposite effect. This is due to it occupied the free volume between polymer chains, which interrupted the electrons. Then, it improved the dielectric strength of the polymers.

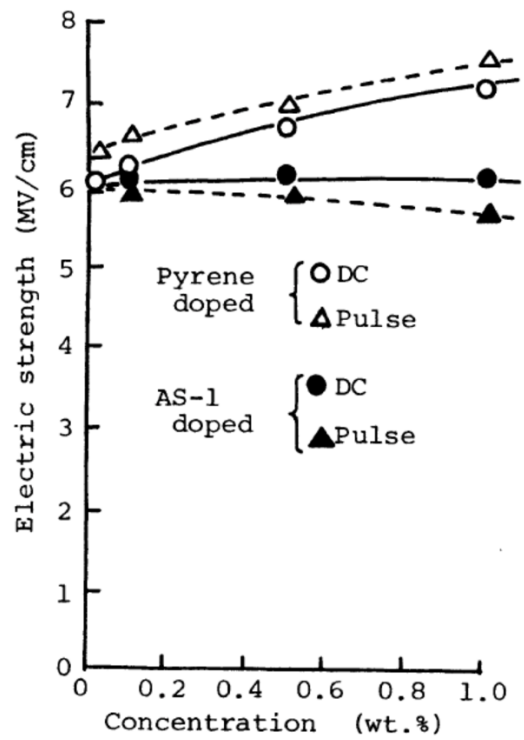


Figure 1-15 The dielectric strength of the polymer with a different additive agent. [42]

Chapter 2

Setup and Experiment Procedure

2.1 Introduction

The knowledge of dielectric materials mentioned in the last chapter can be important information before starting the research. In this chapter, P(VDF-HFP), poly(vinylidene fluoride-co-hexafluoropropylene), was chosen to be the main material for the research because of its good dielectric properties. In addition, adding impurity to polymer thin film is the second perspective of this study. Silane is the main coupling agent in this study. This process can verify the free volume theory and further improve the dielectric property of polymer thin film.

2.2 Experimental Methodology

P(VDF-HFP) is the main material for this research; its density is 1.78g/cm^3 bought from the SIGMA with SKU-Pack Size 427187-100G. The main solvent is N, N-Dimethylformamide (DMF) which bought from Fisher Scientific. Silane (1H, 1H, 2H, 2H-Perfluorooctyltrichlorosilane) is the main additive agent that used in this study; its density is 1.638g/cm^3 and bought from Alfa Aesar company.

This study mainly contained two experimental sections, quench temperature test and the effect from the coupling agent. For the quench temperature test, mainly determined by the microstructure of polymer which may contain a different phase of polymer. Then, based on the experiment, it can find the relationship between the phase and its dielectric properties. Finally, the best quench temperature can be determined for P(VDF-HFP) thin film. The initial quench temperature in our research was derived from the result of the DSC test. Therefore, analyzing the relationship between the dielectric property and the heating process is the first part of the research.

Moreover, after finding the best heating condition for the P(VDF-HFP) thin film, adding silane as a coupling agent is the second approach to further improve the dielectric performance. Overall, the final goal of this study is to improve the energy density of P(VDF-HFP) based thin film and the relationship between the dielectric properties and the microstructure.

2.3 Preparation of Thin Film Sample

2.3.1 Pure P(VDF-HFP) Thin Film

Pure P(VDF-HFP) thin film was mainly used on the quench test experiment. First, dissolved P(VDF-HFP) in the DMF solvent through magnetic stirring under 300 RPM rotation speed for 12 hours. The proportion of P(VDF-HFP) to DMF in this research is 0.2g/10ml. Then, placed the solution into the ultrasonic vibration (Ultrasonic Cleaners, Cole-Parmer Instrument company) for 90 mins to make sure the polymer was dissolved to be uniform and stable. Then, the solution casting process was performed immediately. During the solution casting, dripping 2 ml solution on the glass substrate (Micro slides, 75×25 mm, Corning Incorporated) and dry at 70°C for 8hr. The casting layer would solidify due to the evaporation of the solvent. The thickness of the thin film would be well controlled around 12um with error ± 1 um. Noticed that, the thickness of the thin film related to the concentration of the solution and the amount of solution drip on the substrate. In addition, the flatness of the oven frame needs to be calibrated to make sure the solution can spread on the substrate uniformly.

After obtaining the dry P(VDF-HFP) thin film, the samples were further treated with the following quench process. Different quench temperatures (150°C, 160°C, 170°C, 180°C, 190°C) were selected in this research. Each sample was placed in the preheated oven for 15 min and then immediately put in the ice water. During the quenching process, the film was on the glass substrate. Next, peel off the film under the deionized water. Sample with a higher quench temperature is hard

to peel (especially for the sample above 180 °C); it can use an ultrasonic vibration device to peel off the thin film. Finally, the thin film needs to be dried in room temperature to the next day and then coated the gold electrodes on two sides of the thin film with a diameter of 3mm. The coating process was operated by the gold sputter machine (PELCO SC-6). Finally, the thin film sample was fabricated and ready to do further analysis.

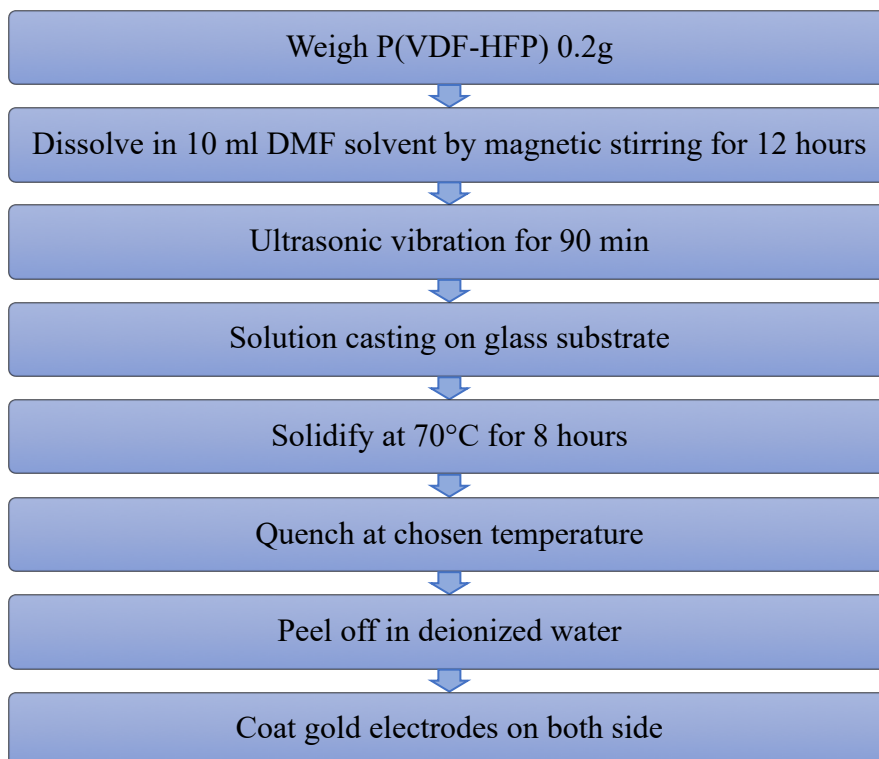


Figure 2-1 Flowchart of the fabrication process.

2.3.2 P(VDF-HFP) Blend with Silane Thin Film.

The process is similar to the previous pure P(VDF-HFP) thin film experiment. First, dissolved P(VDF-HFP) in the DMF solvent through magnetic stirring under 300 RPM rotation speed for 12 hours. The proportion of P(VDF-HFP) to DMF in this research is 0.2g/10ml. Then, silane needs to be dissolved in ethanol before mixing with the P(VDF-HFP) solution, which was stirred using magnetic stirring for 6 hours with 300 rpm rotation speed to make sure it distributed

well in the ethanol solvent. The weight of silane relied on **Table 2.1**. Then, mixed two solutions with magnetic stirring with 300 rpm for 12 hours and follow by ultrasonic vibration for 90 mins. Then, fabricating the thin film by solution casting immediately with 2 ml of the mixed solution drip on the glass substrate (Micro slides, 75×25 mm, Corning Incorporated) and dry at 70°C for 8hr. The casting layer would solidify due to the evaporation of the solvent. The thickness of the thin film would be well controlled around 10um with error $\pm 1\mu\text{m}$. Overall, the solution casting process was roughly the same with pure P(VDF-HFP) thin film but different in the thickness.

Then, quenching the thin film at the best quench temperature, which obtained from the pure P(VDF-HFP) thin film experiment. The quenching process is identical to the pure P(VDF-HFP) thin film. Next, peel off the thin film in the deionized water. However, the sample with silane was easy to peel compared to the pure P(VDF-HFP) thin film. Therefore, all the samples do not need to be peeled under ultrasonic vibration. Finally, the thin film was dried at room temperature to the next day and then coated the gold electrodes on two sides of the thin film with a diameter of 3mm. The coating process was operated by the gold sputter machine (PELCO SC-6). Then, the thin film sample was finished and ready to do further analysis.

Wt.% of Silane	P(VDF-HFP) (g)	Silane (g)	Ethanol (ul)	DMF (ml)
0.2	0.2	0.0004	66.6	10
0.4	0.2	0.0008	133.3	10
0.6	0.2	0.0012	200	10
0.8	0.2	0.0016	266.6	10
1.0	0.2	0.0020	333.3	10

Table 2-1 Weight ratio of silane in P(VDF-HFP).

2.4 Characterization Method

Differential Scanning Calorimeter (DSC) was used in this study to characterize the thermal properties of all the samples by using a TA instrument, Inc. DSC250 (shown in **Figure 2-2**). All the polymer thin film was sealed in the aluminum pan with the mass between 12 to 15 mg. During the test, the same type of empty pan was placed in the machine chamber to serve as a reference. The test started from -90°C to 250°C with a temperature rate of $10^{\circ}\text{C}/\text{min}$. Then, maintaining the temperature at 250°C for 1 minute and decreasing the temperature to -90°C with a rate of $10^{\circ}\text{C}/\text{min}$. The results of the test will be demonstrated in the next chapter.



Figure 2-2 Differential Scanning Calorimeter (DSC) machine.

Impedance analyzer (Agilent 4294A precision) was used in this study to characterize dielectric properties (shown in **Figure 2-3**). The frequency range used in this study was from 100 Hz to 1M Hz. The number of frequency points, measurement function and source were set to 801, Cp-D, 500 mV/div. respectively. First of all, the machine was calibrated under both short and open conditions before utilization. All the tests were operated under the room temperature ($\sim 24^{\circ}\text{C}$). The

value of capacitance (C) and dielectric loss ($\tan\delta$) at each frequency can be obtained. Then, the dielectric constant (ϵ) of the sample can be calculated using equation (1.2). Therefore, the result shown in the next chapter will be the relationship between the dielectric constant and the frequency.



Figure 2-3 Agilent 4294A impedance analyzer

The polarization-electric field loop (P-E loop) was a by using a Radiant Precision LC100 system. In addition, the machine of high voltage supply was bought from Trek with model 610D (shown in **Figure 2-4**). All the tests were operated by placing the sample in silicone oil to prevent short circuits by the air. The machine can connect with the laptop and be controlled by the software “Vision”; it can also plot P-E loop for our further analysis. The value of displacement (\vec{D}) and polarization (\vec{P}) were very close due to the high permittivity of the thin film. Then, the energy density can be calculated by equation (1.18). Besides that, if only connect the high voltage supply to our sample, the dielectric strength can be examined by manually control the voltage output. When doing the dielectric strength test, the limitation of current was set to 600 μA , meaning that the sample was regarded as an electric breakdown if the current over 600 μA .



Figure 2-4 Precision-LC100 system and H.V. Supply Amplifier.

Chapter 3

Study of P(VDF-HFP) Thin Film

3.1 Test Condition

As discussed in **Chapter 2**, the condition of the quench treatment of pure P(VDF-HFP) thin film was the first perspective in this study. **Figure 3-1** showed the DSC result of pure P(VDF-HFP) thin film without a quench. It can be found that the endothermic peak was at around 140°C and the exothermic peak was at around 105°C. The endothermic peak can be considered as the melting point of our sample and the exothermic peak can be considered as the crystallization process. Therefore, the important information that we can obtain from this is that the quench temperature has to be over 140°C. In this condition, we can make sure the polymer was transferred to a liquid-like phase and get rid of the crystalline phase. Therefore, the following dielectric properties test will be based on this DSC result. The quench temperature at 150°C, 160°C, 170°C and 180°C were chosen for the following examination.

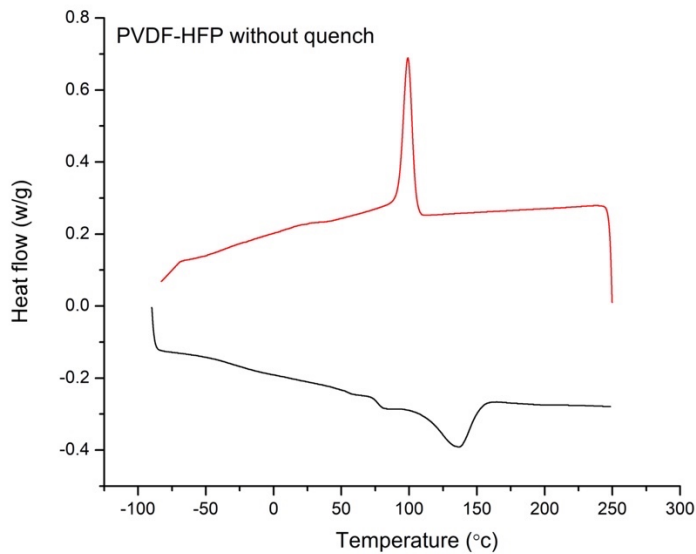


Figure 3-1 DSC of pure P(VDF-HFP) thin film.

3.2 Study of P(VDF-HFP) Thin Film

3.2.1 Frequency Dependency of Dielectric constant and Loss

The real part of the relative dielectric constant of pure P(VDF-HFP) with different quench temperatures showed in **Figure 3-2**. It can be found that the thin film quench at 160°C has a better/higher dielectric constant compared to other quench temperature. At 100 Hz frequency, the dielectric constant for the quench temperature of 150°C, 160°C, 170°C and 180°C are 13.4, 14.3, 13.9 and 13.8, respectively (shown in **Figure 3-4**). Moreover, when the frequency at around 10^5 Hz, the dielectric constant of the sample with the quench temperature at 160°C and 180°C are very close. This explained the sample have different dielectric behavior at different frequency range. Therefore, from the viewpoint of improvement of permittivity, different quench temperature can be an important factor for P(VDF-HFP) thin film.

Figure 3-5 showed the dielectric loss among the samples; the sample quench at 160°C has the highest value of the dielectric loss. The dielectric loss for the sample quench at 160°C and 170°C is very close at the low frequency. This also happened in the sample quench at 150°C and 180°C, too. Meanwhile, the sample quench at 180°C has a relatively high dielectric loss at a higher frequency range.

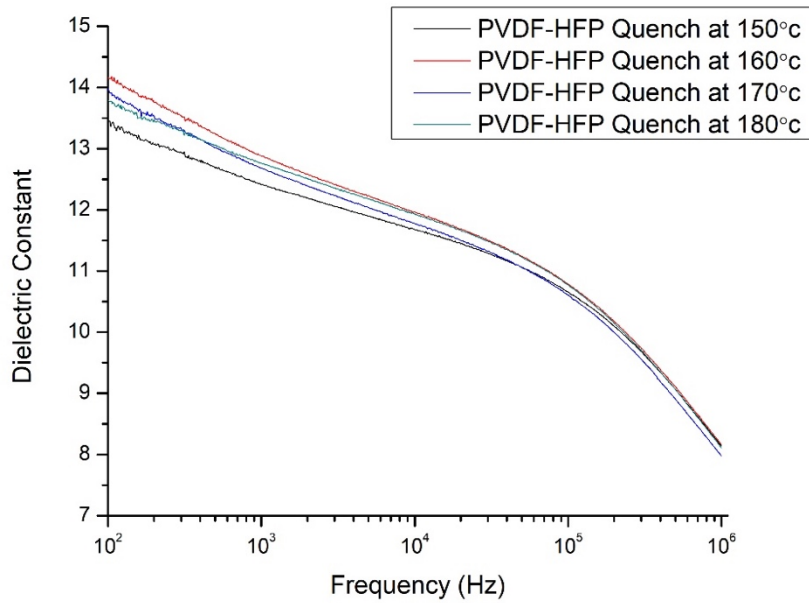


Figure 3-2 Dielectric constant of pure P(VDF-HFP) thin film with different quench temperature.

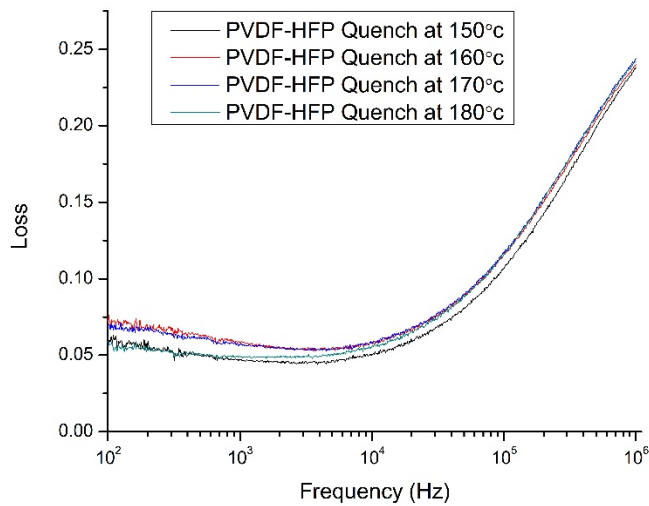


Figure 3-3 Dielectric loss of pure P(VDF-HFP) thin film with different quench temperature.

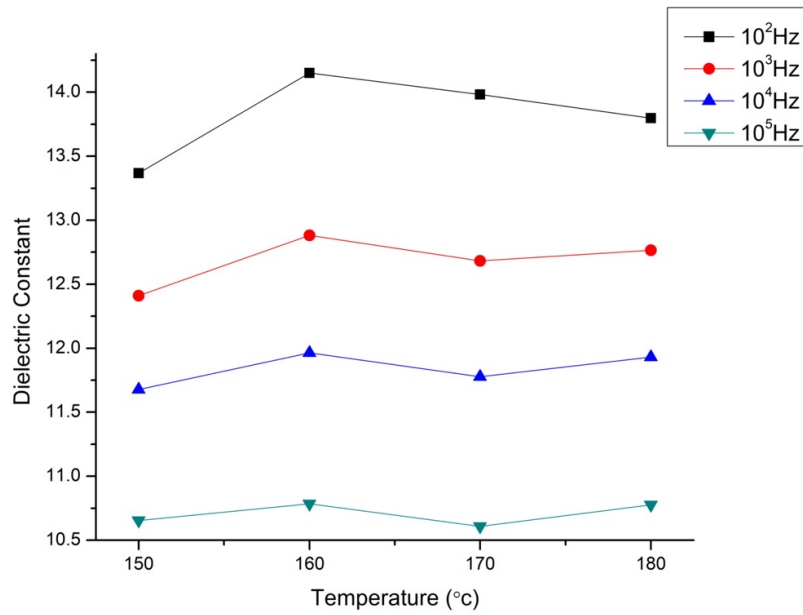


Figure 3- 4 Dielectric constant of pure P(VDF-HFP) thin film in different quench temperature and sorted by frequency.

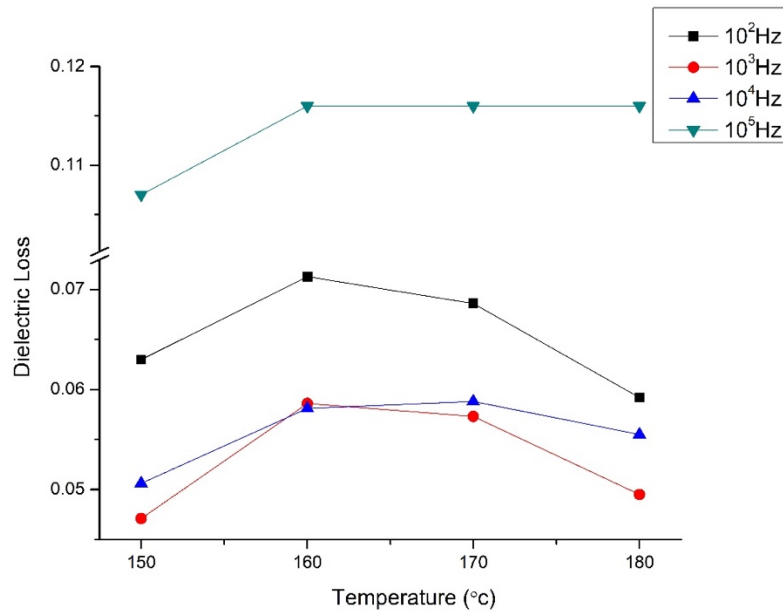


Figure 3-5 Dielectric loss of pure P(VDF-HFP) thin film in different quench temperature and sorted by frequency.

3.2.2 Dielectric Breakdown Strength

As mentioned in **Chapter 2**, the breakdown strength can be measured by connecting the sample to the power supply. Then, manually increasing the voltage until the current exceeds a set value. In this study, we defined the 600uA is the critical point. Therefore, from the experiment, the breakdown strength can be grained. After that, the data needs to organize through Weibull distribution. Based on the Weibull plot, we defined the value of dielectric strength while the thin films have 63.2% cumulative failure probability. Therefore, the dielectric breakdown field strength can be further quantified and analyzed.

Figure 3-6 showed the Weibull plot of the P(VDF-HFP) thin film with different quench temperatures. The heating duration was 15min and immediately quench in the ice water. Obviously, the dielectric breakdown strength gradually decreases with increasing temperature. Moreover, the slope can demonstrate how to date distribution. If the samples with a smaller slope, it had more probability to breakdown far away from the value that we calculated, meaning the date has a wider range. Based on this concept, the sample quench at 150°C, 160°C and 180°C have very similar slope; however, from the simple quench at 170°C the slope was obviously smaller than higher temperature sample. It explained that the microstructure of the sample may not as uniform as other samples. It can be an important factor to influence the reliability of the sample.

Besides that, when we consider the final value of the dielectric breakdown field strength, it gradually decreases with increasing quench temperature. The possible reason may be the crystallinity of the sample. The endothermic peak of P(VDF-HFP) is 140°C but the peak is wide enough to cover 150°C and 160°C (shown in **Figure 3-1**). This explained the sample quench at 170°C and 180°C have a similar value of dielectric breakdown field strength. From this viewpoint, the crystallinity needs to be examined by further analysis.

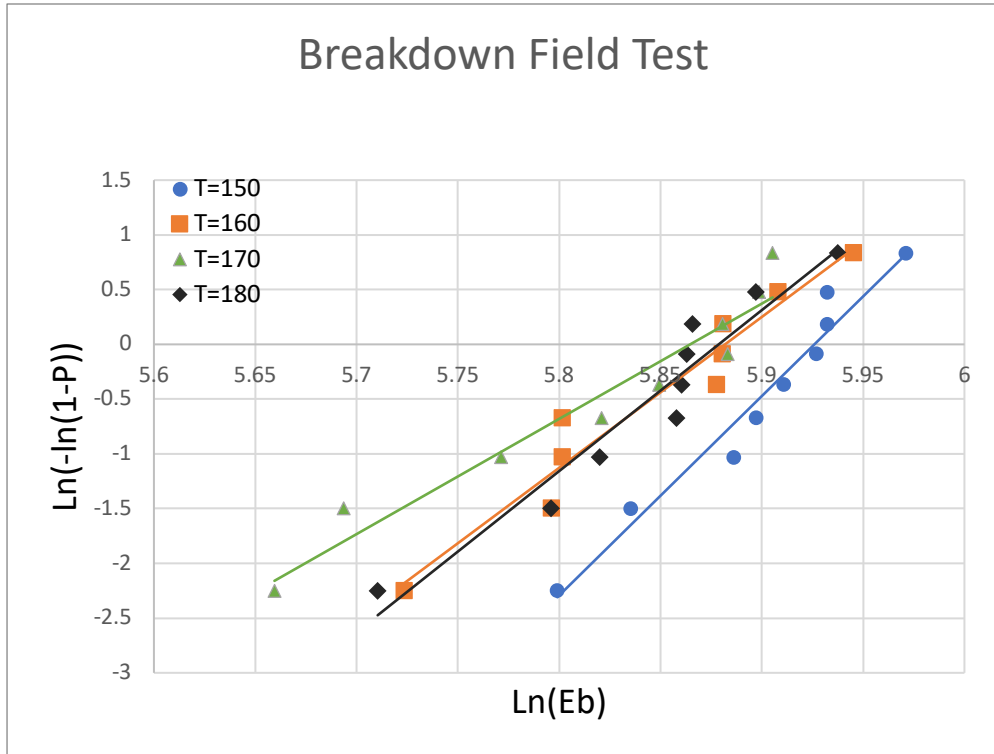


Figure 3-6 Weibull distribution plot for dielectric breakdown strength of the samples with different quench temperature.

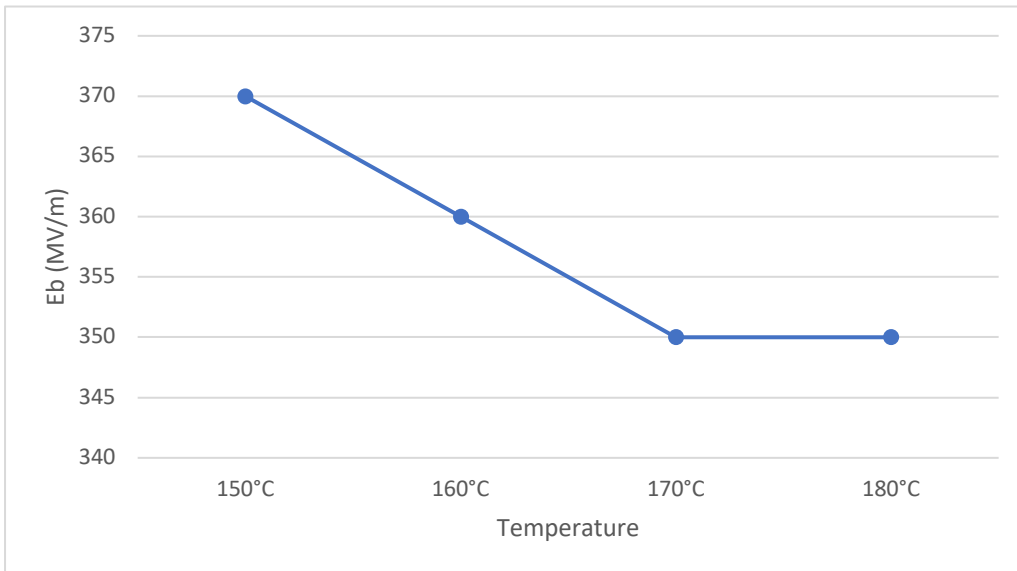


Figure 3-7 Dielectric breakdown strength versus quench temperature for P(VDF-HFP).

3.2.3 Polarization-Electric Field Hysteresis Loops and Energy Density

Figure 3-8~3-11 showed the polarization-electric field (P-E) loop for all samples. The loop was measured at 100 Hz and the electric field gradually increased with 500 KV/cm until the breakdown field subtracted 500 KV/cm in order to protect the machine. It showed the P_{max} increased with increasing electric field and the loop area becomes larger and larger, meaning that the thin film would lose more energy when applied under the high electric field. Then, for the next part, it will compare the P-E loop between different samples under the maximum electric field and the energy density.

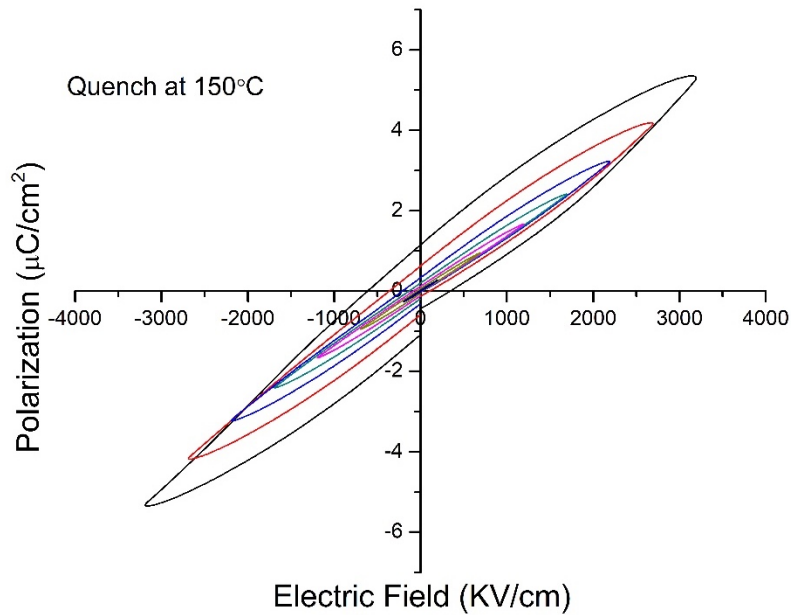


Figure 3-8 P-E loop of P(VDF-HFP) thin film quench at 150°C.

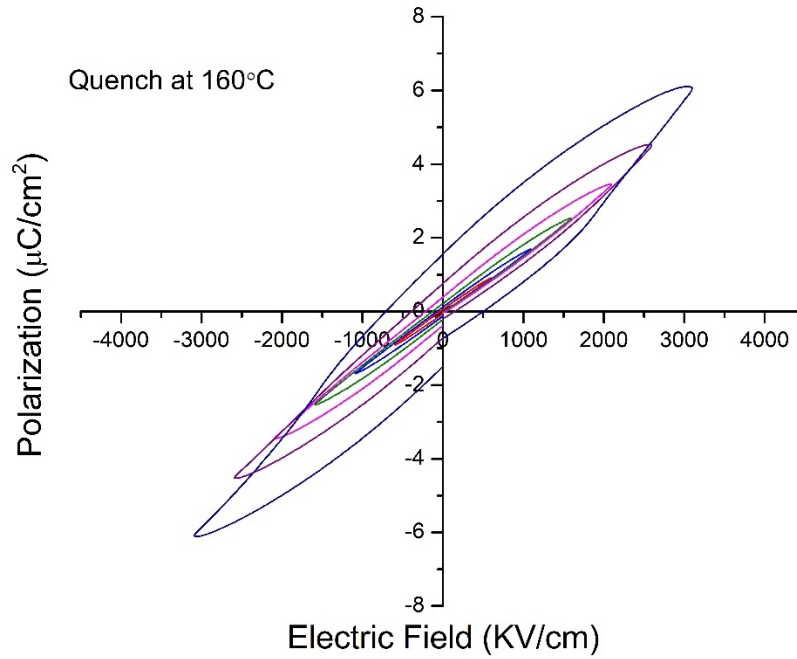


Figure 3-9 P-E loop of P(VDF-HFP) thin film quench at 160°C.

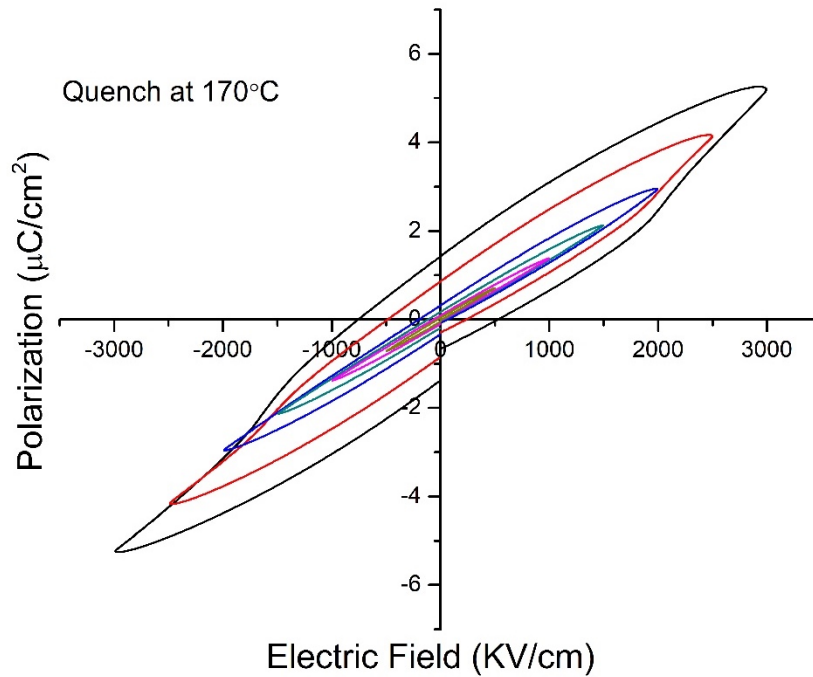


Figure 3-10 P-E loop of P(VDF-HFP) thin film quench at 170°C.

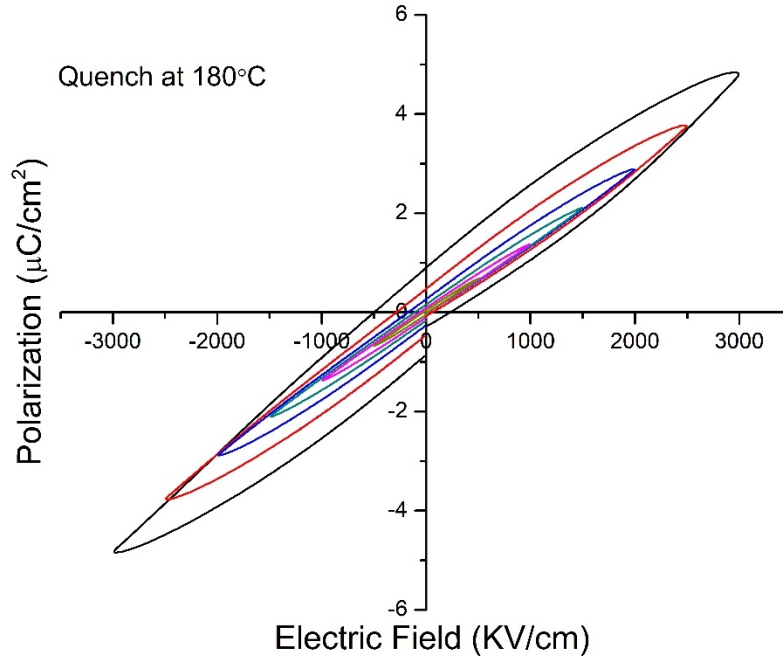


Figure 3-11 P-E loop of P(VDF-HFP) thin film quench at 180°C.

Figure 3-12 showed the P-E loop of the P(VDF-HFP) thin film quench at different temperatures under 2000 and 3000 KV/cm external electric field. It can be found that the P_{max} reached the maximum for the sample quench with temperature 160°C. Plus, the P_{max} of the samples quench at 170°C and 180°C are almost the same. And the sample quench at 150°C has relatively small P_{max} . The result of the P-E loop is very similar to the previous dielectric constant analysis. The sample has better dielectric constant when quenching at 160°C; then, the 150°C sample is not as good as 170°C and 180°C sample. Interestingly, the samples quench at 170°C and 180°C were equipped with similar dielectric constant, dielectric breakdown strength and P-E loop. In addition, the dielectric loss was similar at high frequency range. Therefore, the result of the P-E loop can prove the result from the previous dielectric test.

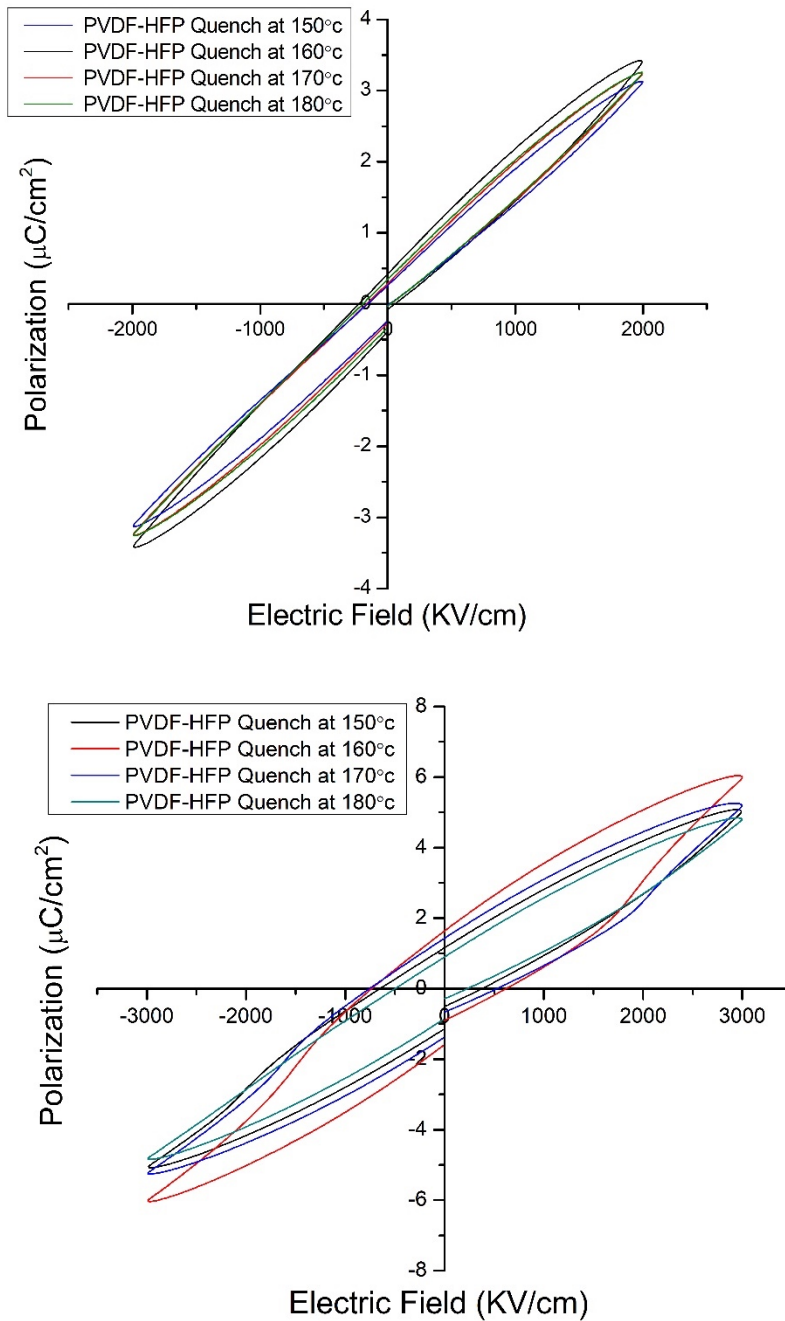


Figure 3-12 P-E loop of pure P(VDF-HFP) thin film for different quench temperatures under 2000KV/cm (top) and 3000KV/cm (bottom) electric field.

Based on the dielectric breakdown strength result, the samples have different abilities to sustain the electric field. Therefore, in order to measure the best condition of the specimens, analyzing the P-E loop on the maximum electric field was required. **Figure 3-13** showed the P-E

loop test when the sample reached the dielectric breakdown strength. The electric field of test condition for the quench at 150°C, 160°C, 170°C and 180°C were 320, 310, 300 and 300 (MV/m). In this test, applied the external electric field was the maximum condition subtracted 50 (MV/m) to protect the machine. From the result, it can be found that the sample quench at 160°C has higher permittivity. Although it is not the best sample to sustain the external electric field, it can release more energy when discharging. Then, compared with the electric field of 200 (MV/m), the P-E loop of sample quench at 170°C and 180°C separated under this condition. The possible reason may be the molecular weight of the sample. When the quench temperature increase, the polymer chains may break and generate microdefects. That phenomenon would decrease the permittivity of the polymer.

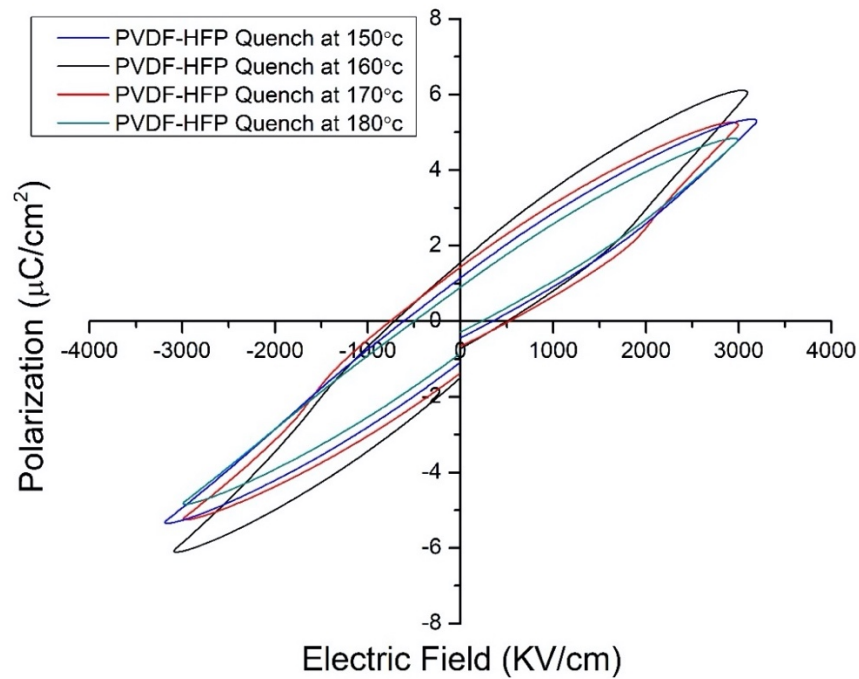


Figure 3-13 P-E loop of pure P(VDF-HFP) thin film for different quench temperature under its maximum electric field.

Figure 3-14~3-16 are the result of the energy density and efficiency calculated by the previous maximum P-E loop analysis. The energy density of charge and discharge reached the maximum for the sample quench at 160°C, which is 12.0 (J/cm³) and 6.3 (J/cm³), respectively. Then, the efficiency of all thin films was from 45% to 53%, which was calculated by discharge density/charge density. Then, it exhibited a significant difference when raising the quench from 160°C to 170°C. The efficiency decreased around 8% and kept the same value of efficiency to 180°C, which explained 170°C and 180°C sample perhaps have very similar microstructure. Finally, the result of the energy density can prove the quench temperature influence the dielectric property. Obviously, pure P(VDF-HFP) thin film quench at 160°C can reach the best performance of energy storage in this research. Besides, **Figure 3-17~3-19** showed energy density under different electric fields.

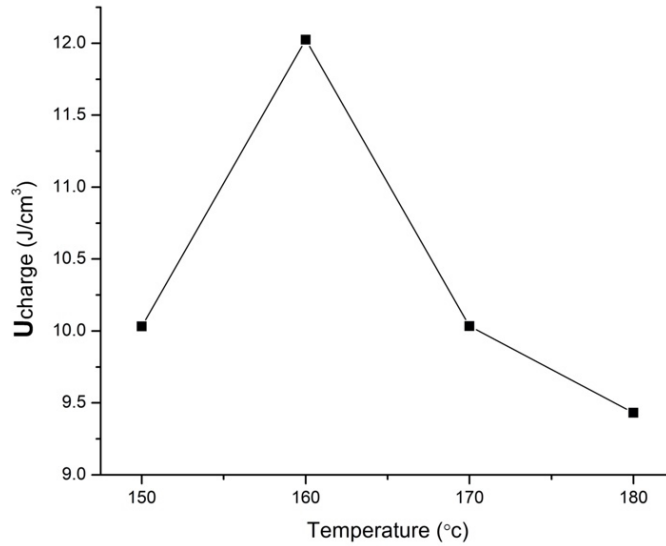


Figure 3-14 Energy density of pure P(VDF-HFP) thin film with different quench temperatures for the charging process.

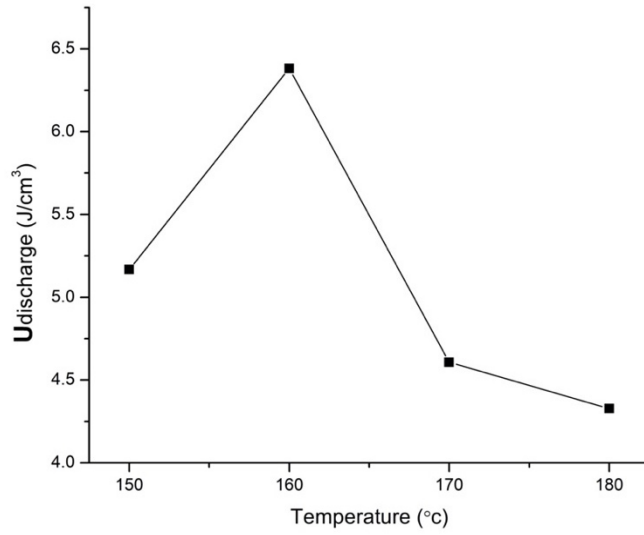


Figure 3-15 Energy density of pure P(VDF-HFP) thin film with different quench temperatures for the discharge process.

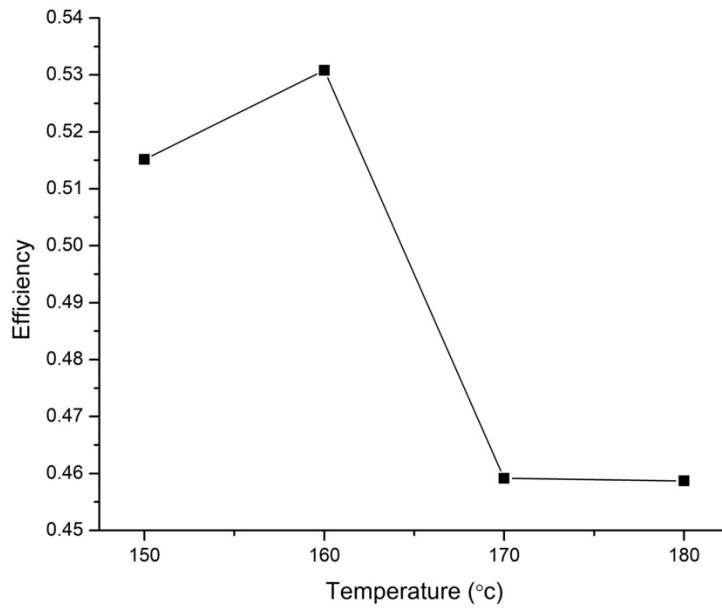


Figure 3-16 Efficiency of pure P(VDF-HFP) thin film with different quench temperature.

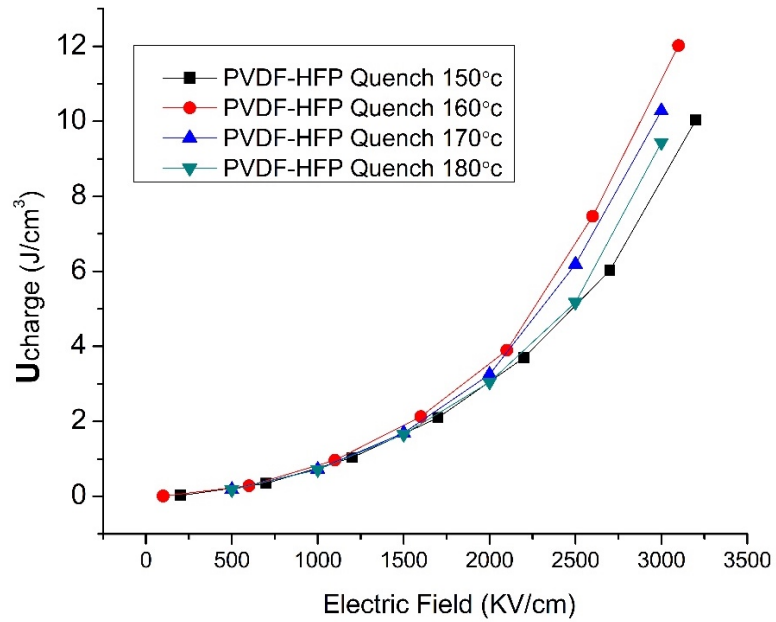


Figure 3-17 Energy density of pure P(VDF-HFP) thin film with different quench temperatures for the charging process under different electric fields.

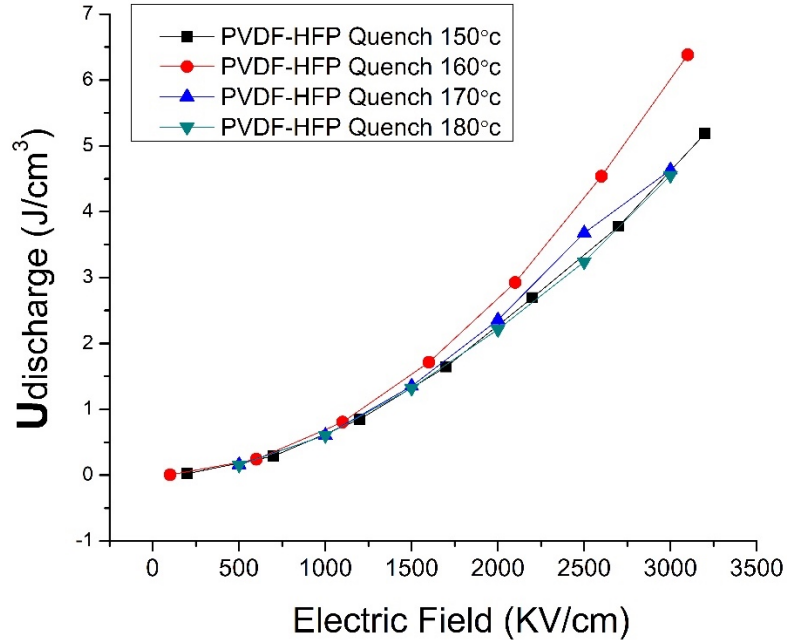


Figure 3-18 Energy density of pure P(VDF-HFP) thin film with different quench temperatures for the discharge process under different electric fields.

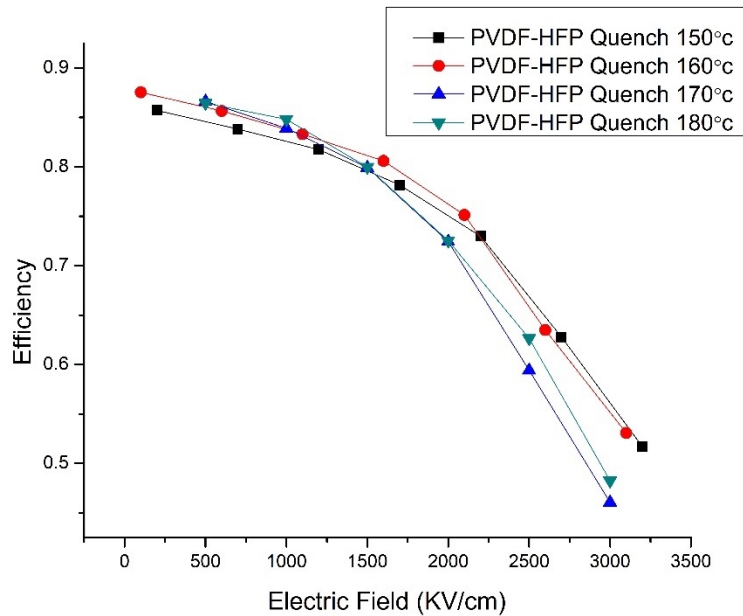


Figure 3-19 Efficiency of pure P(VDF-HFP) thin film with different quench temperature under different electric fields.

3.2.4 Differential Scanning Calorimeter (DSC) Test

DSC can provide the thermal property of the specimen especially when the polymer has a different phase. **Figure 3-20~3-21** showed the result of the DSC test for the P(VDF-HFP) thin film with different quench temperatures. The weight of the polymer thin film was from 10mg to 15mg. The heating process was from -90°C to 250°C and cool from 250°C to -90°C with a rate of $10^{\circ}\text{C}/\text{min}$. Then, the data was organized to the range from -30°C to 250°C for the heating process and -50°C to 230°C for the cooling process. However, the black and red curves have an obvious second peak different from other samples. That was caused by the second phase of the P(VDF-HFP). The possible phase is the α phase of P(VDF-HFP). As mentioned in **Ref 43**, the β phase of P(VDF-HFP) has lower permittivity (~ 13) than α phase (~ 14). This may be the reason that the

sample quench at 150°C has a lower dielectric constant than other samples. Then, the sample quench at 170°C and 180°C have a very similar DSC result. Both of the samples have only the β phase. Therefore, it assumed that the dielectric properties can be very similar, which proved again the result that showed above. Moreover, the possible reason is that quenching at higher temperatures may generate more microdefects and further decrease the permittivity and dielectric breakdown strength.

Figure 3-21 showed the heat flow during the cooling process. All the exothermic peaks were perfectly located at the same temperature. Then, **Figure 3-22** showed the enthalpy of the DSC result. Higher quench temperature would cause the sample to have a lower percentage of crystallization and absorb less heat. Therefore, the enthalpy of endothermic peak decrease with increasing quench temperature.

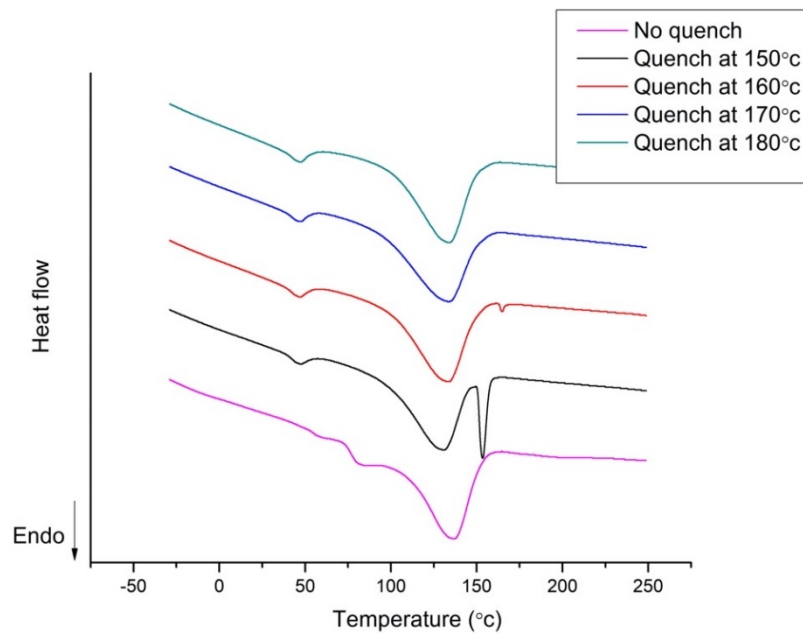


Figure 3-20 The heating process of DSC for pure P(VDF-HFP) thin film quench at different temperatures.

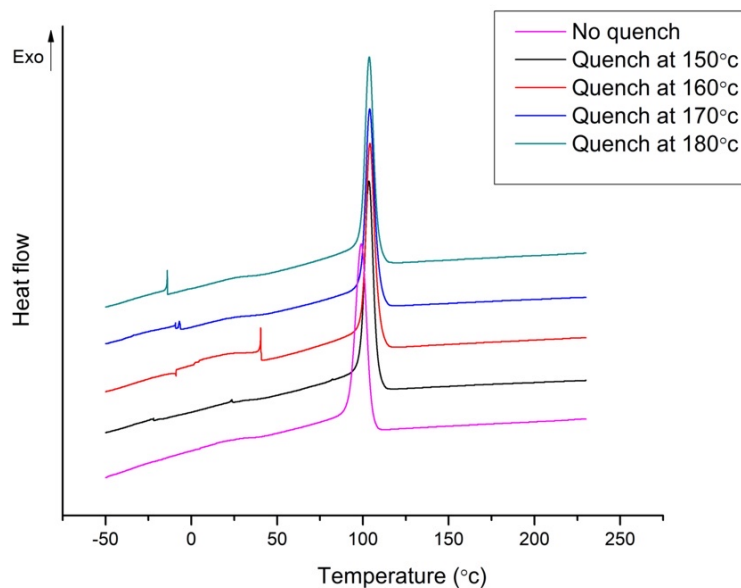


Figure 3-21 The cooling process of DSC for pure P(VDF-HFP) thin film quench at different temperatures.

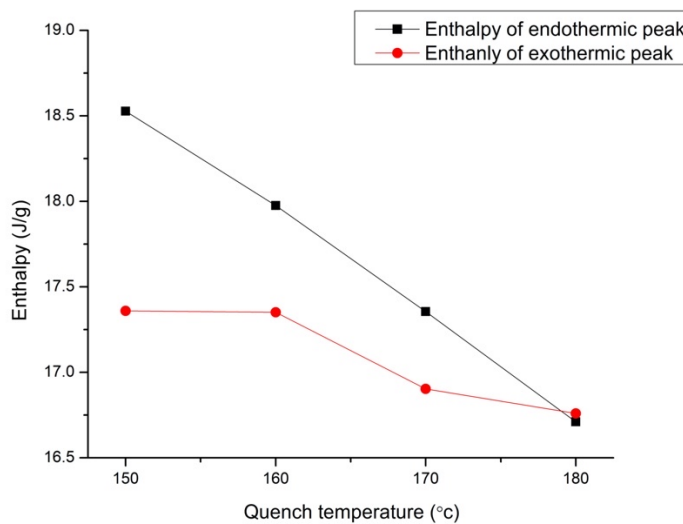


Figure 3-22 Enthalpy of the P(VDF-HFP) thin film with different quench temperature calculated by the DSC result.

3.3 Study of P(VDF-HFP) with Silane Thin Film

3.3.1 Frequency Dependency of Dielectric constant and Loss

Figure 3-23 showed the dielectric constant of the P(VDF-HFP) thin film with different amounts of silane. All the samples were prepared by the quenching process which is identical to the sample prepared in the last section and the temperature was set to 160°C. From the result of the permittivity test, the dielectric constant increase with an increasing amount of the silane initially and then rapidly decreased. The thin film with 1wt% silane even worse than the original sample. Then, the sample with 0.6wt% and 0.8wt% have better dielectric constant than the film in other concentrations. Compared to the original quench sample, it improved around 4% at 100Hz and 7% at 10,000 Hz (shown in **Figure 3-25**). However, the sample with 0.6wt% of silane has the highest dielectric loss among the test, which was not good for the energy density. Overall, from this permittivity examination, it can confirm that adding silane can change the dielectric properties of the P(VDF-HFP).

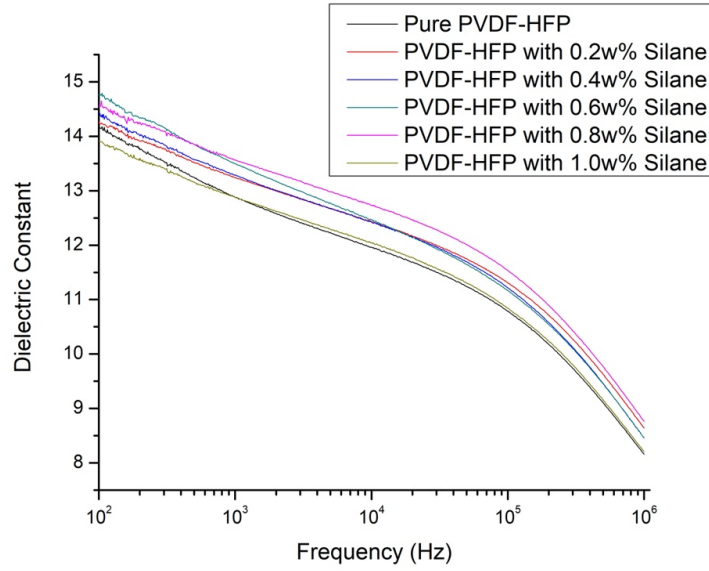


Figure 3-23 Dielectric constant of P(VDF-HFP) thin film with different concentrations of silane.

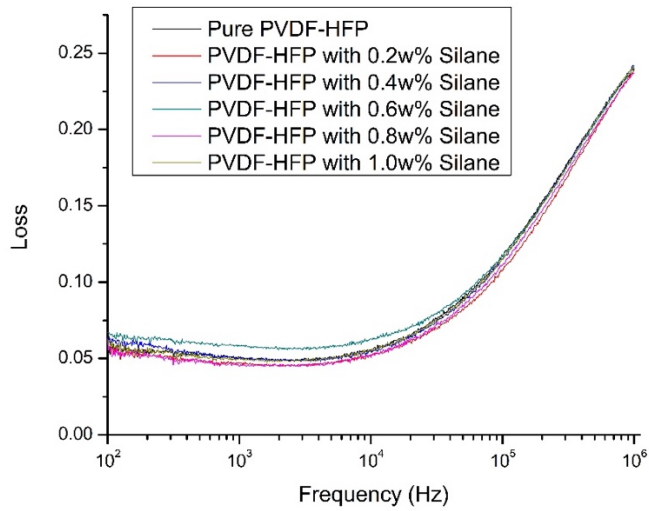


Figure 3-24 Dielectric loss of P(VDF-HFP) thin film with different concentrations of silane.

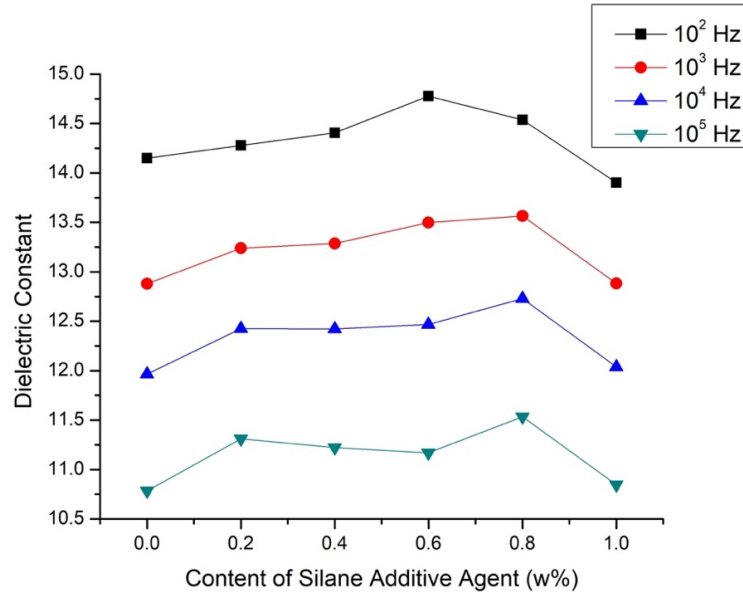


Figure 3- 25 Dielectric constant of P(VDF-HFP) thin film with different concentrations of silane and sorted by frequency.

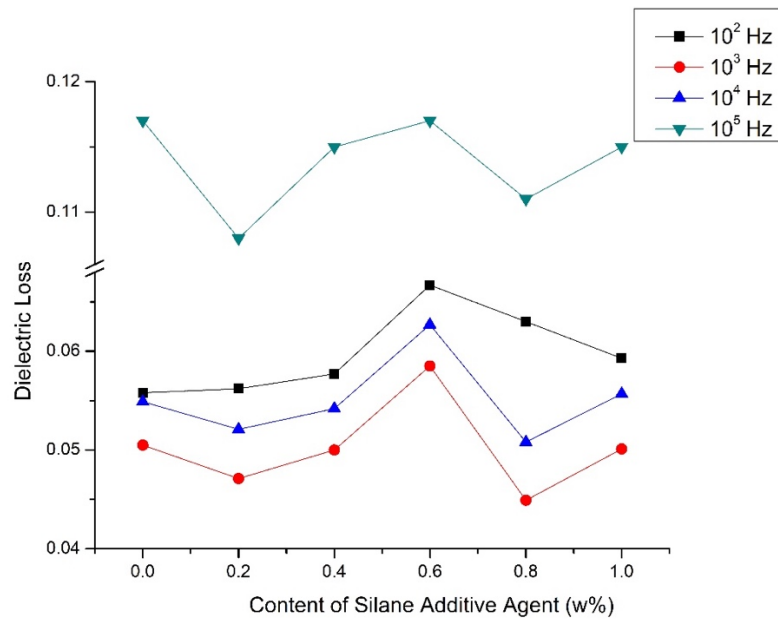


Figure 3-26 Dielectric loss of P(VDF-HFP) thin film with different concentrations of silane and sorted by frequency.

3.3.2 Dielectric Breakdown Strength

The test condition in this section was the same as the previous pure P(VDF-HFP) test. It was defined as a breakdown when the current exceeded 600uA. **Figure 3-27~3-28** showed the result of the breakdown test. The dielectric breakdown strength increased with an increasing amount of silane and start to decrease when it reached 0.6wt% of silane. From the result, it can be calculated that the dielectric breakdown strength can be improved about 20%. However, the dielectric strength decreased around 20% when the concentration reached to 1.0wt%. The possible reason may relate to the free volume theory. This additive agent filled up the free space between polymer chains. Then, the extra molecular can help polymer sustain more electric field than the previous condition. Therefore, from the result of the dielectric breakdown test, it can verify that adding silane can exert positive influence when fabricating high energy density dielectric films.

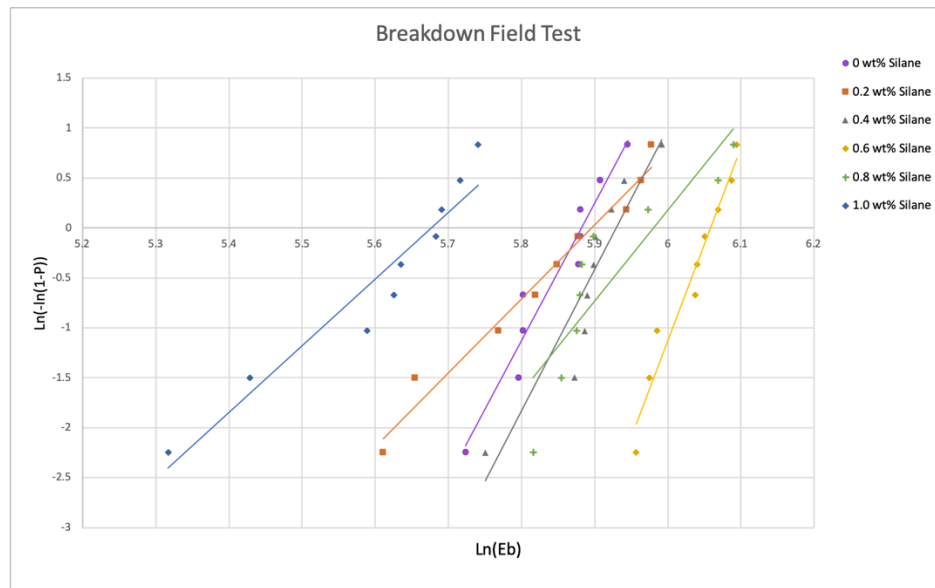


Figure 3-27 Weibull distribution plot for dielectric breakdown strength of the samples with different concentrations of silane.

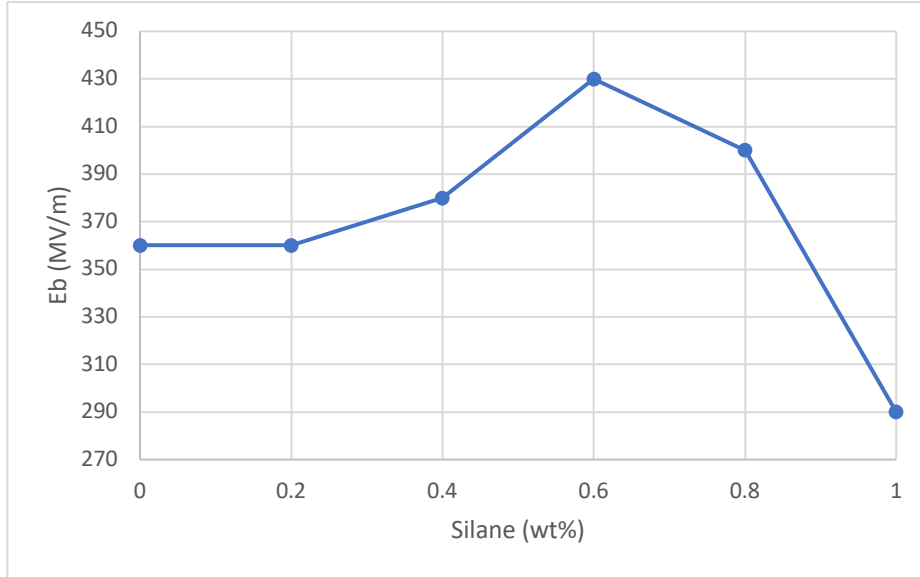


Figure 3-28 Dielectric breakdown strength of P(VDF-HFP) thin film with different concentrations of silane.

3.3.3 Polarization-Electric Field Hysteresis Loop and Energy Density

Figure 3-29~3-33 showed the polarization-electric field (P-E) loop for the P(VDF-HFP) thin film with different content of the silane (0.2wt%~1.0wt%). All the measurements were tested under 100 Hz and the electric field gradually increased with 500 KV/cm until the breakdown field subtracted 500 KV/cm in order to protect the machine. Therefore, all the test conditions were identical to the previous pure P(VDF-HFP) thin film. From the P-E loop result, it can be found that the thin film contained 0.4wt%~0.8wt% exhibited strong ferroelectric loop, meaning the loops were equipped with a very big value of loss during the high electric field. However, the ferroelectricity reached the maximum when the concentration is 0.6wt%. It can be proved by observing the value of the coercive field.

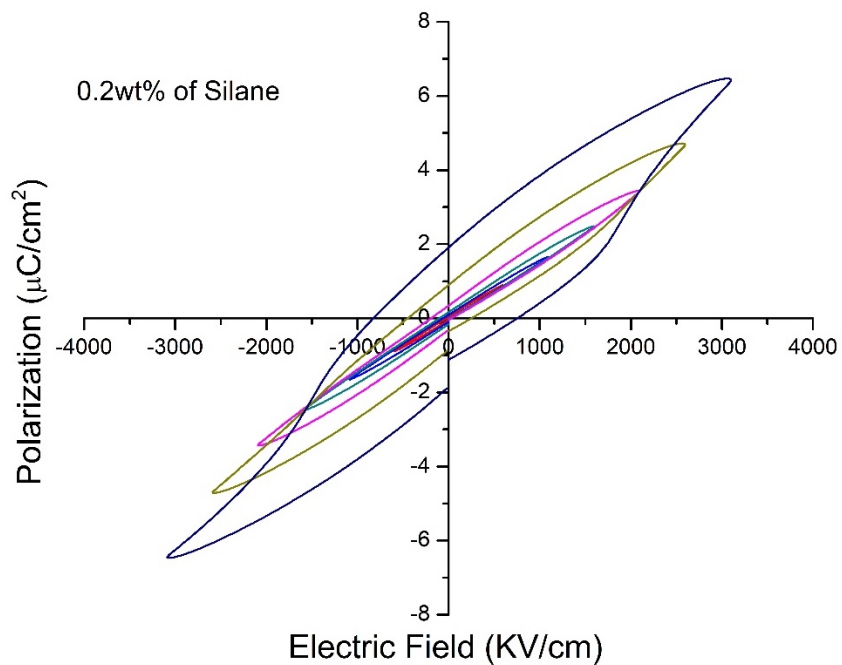


Figure 3-29 P-E loop of P(VDF-HFP) thin film with 0.2wt% of silane.

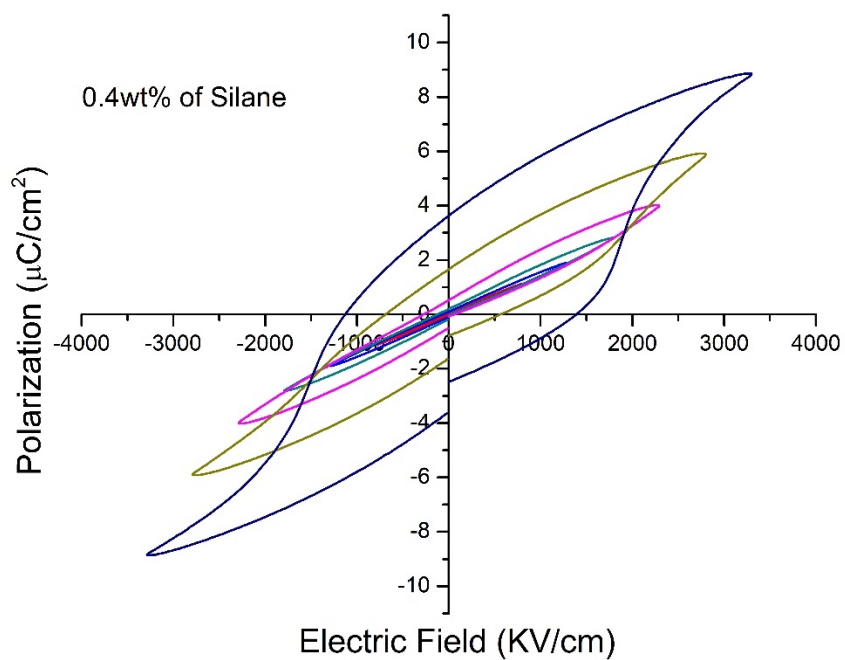


Figure 3-30 P-E loop of P(VDF-HFP) thin film with 0.4wt% of silane.

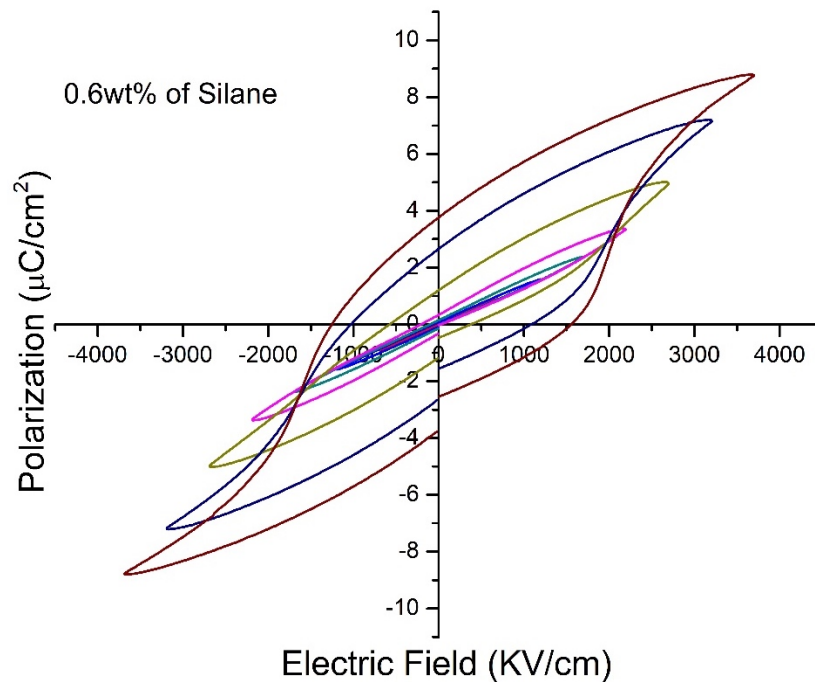


Figure 3-31 P-E loop of P(VDF-HFP) thin film with 0.6wt% of silane.

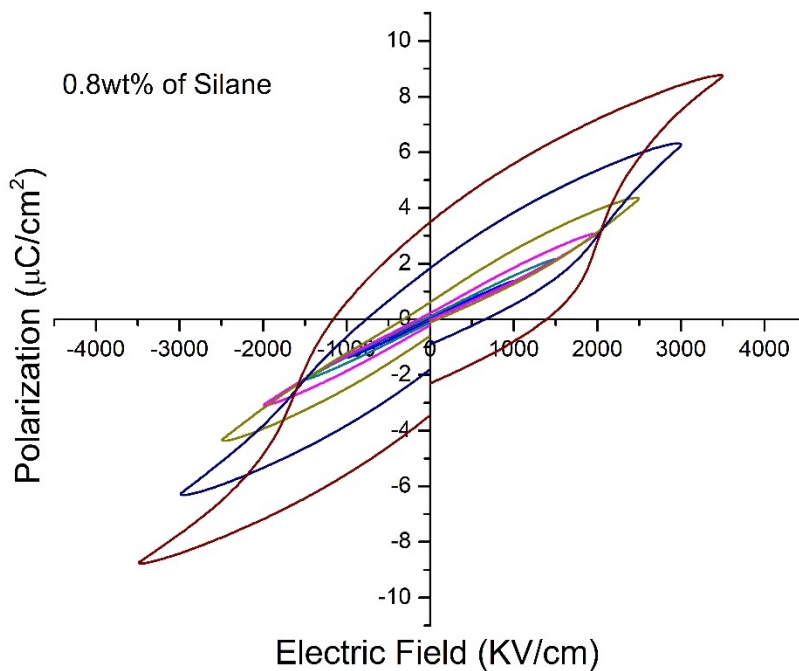


Figure 3-32 P-E loop of P(VDF-HFP) thin film with 0.8wt% of silane.

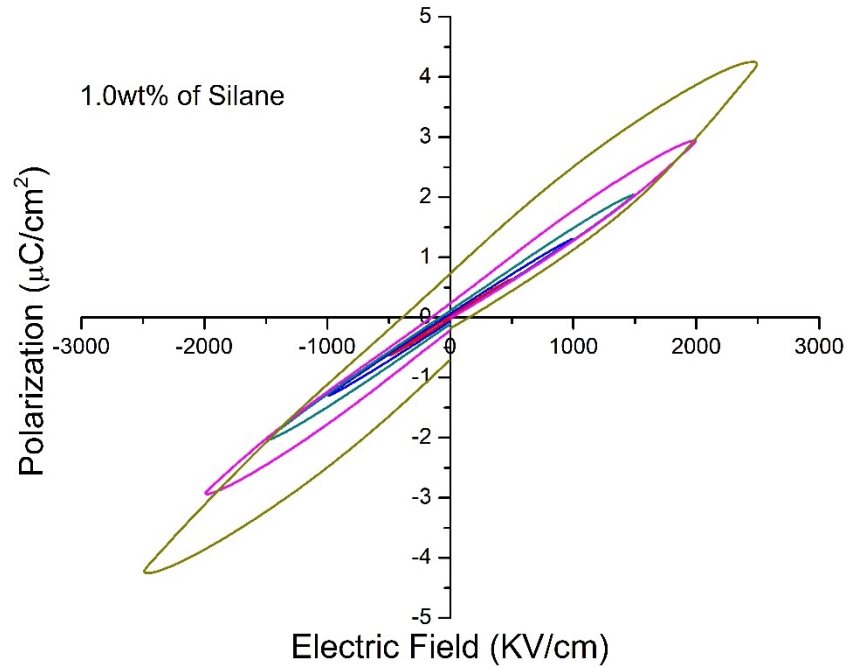


Figure 3-33 P-E loop of P(VDF-HFP) thin film with 1.0wt% of silane.

Figure 3-34 showed the sample under the same external electric field with different concentrations of silane. This result can verify the result of the permittivity test. The slope of the P-E loop can reflect the permittivity of the sample. Higher permittivity has a higher slope of P-E loop. Moreover, the dielectric loss of the sample is very close under the 2000MV/cm external electric field.

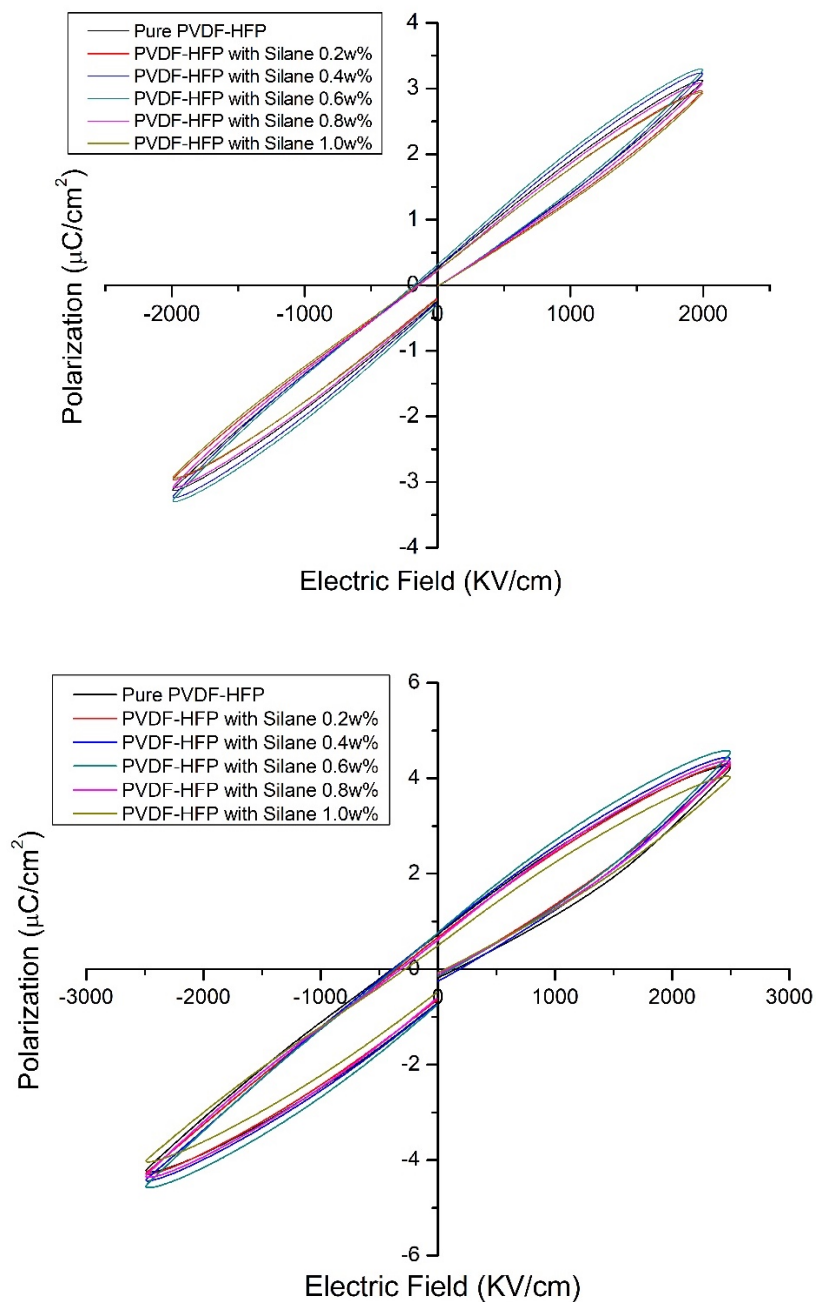


Figure 3-34 P-E loop of P(VDF-HFP) thin film with different concentrations of silane under 2000 KV/cm (top) and 3000KV/cm (bottom) electric field.

Figure 3-35 showed the P-E loop when the sample under its maximum electric field. The sample with 0.4wt%~0.8wt% of silane has very different results from other samples. The applied electric field was very similar among samples with 0.2wt%~0.8wt% silane and the pure sample.

However, the sample with 0.4wt%~0.8wt% silane exhibited strong ferroelectric properties. It seemed the silane change the dielectric property of the P(VDF-HFP) from linear to ferroelectric. Then, when the concentration of silane up 1.0wt%, it cannot get the result under the higher electric field due to the lower dielectric breakdown field.

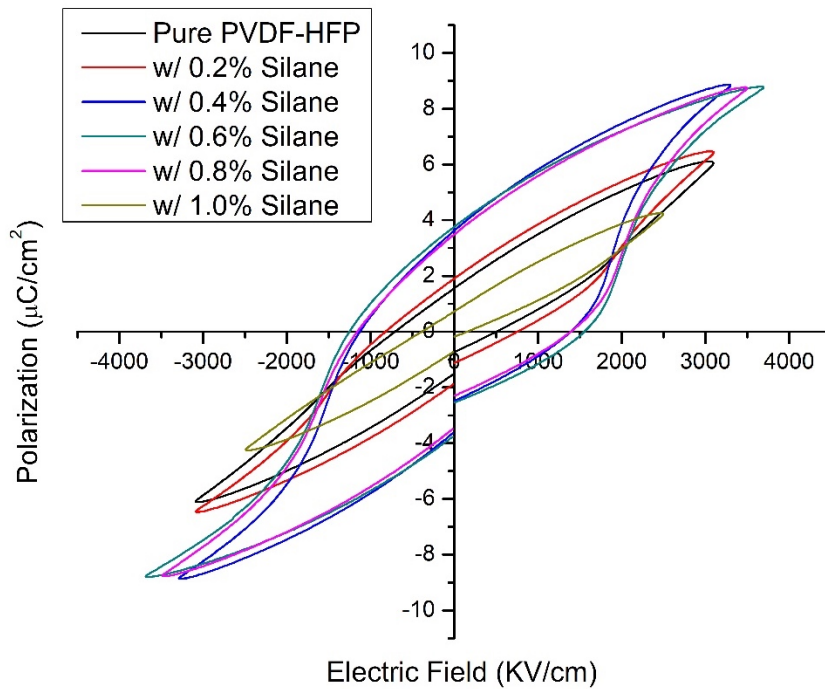


Figure 3-35 P-E loop of P(VDF-HFP) thin film with different concentrations of silane under its maximum electric field.

Based on the P-E loop of the sample under its maximum electric field that is lower than E_b , the energy density and the efficiency can be calculated (shown in **Figure 3-36~3-38**). From the result of the discharge analysis, it can be found that the energy density increased around 18% for the 0.8wt% sample. However, the efficiency decreased a lot, which was around 30%. This is due to high ferroelectricity; most of the energy released by heat. From this result, it proved that the energy density of the P(VDF-HFP) thin film can be improved by adding silane as a coupling

agent but scarified the efficiency at the same time. Besides, **Figure 3-39~3-41** showed the energy density of silane thin film under a different electric field.

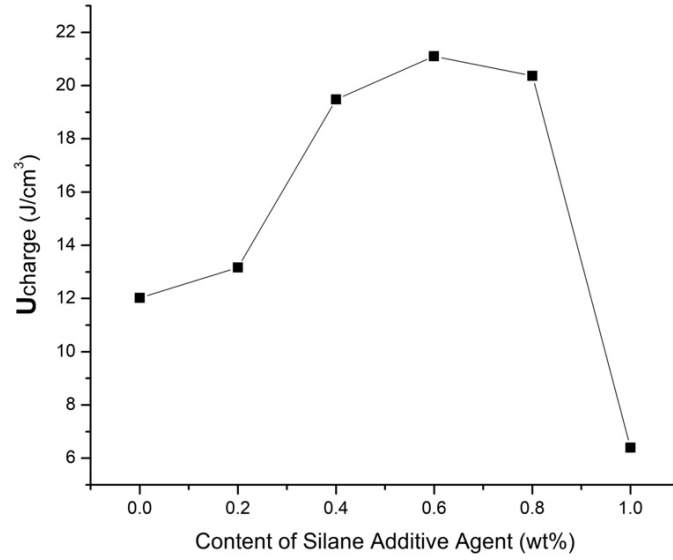


Figure 3-36 Energy density of P(VDF-HFP) thin film with different concentrations of silane for the charging process.

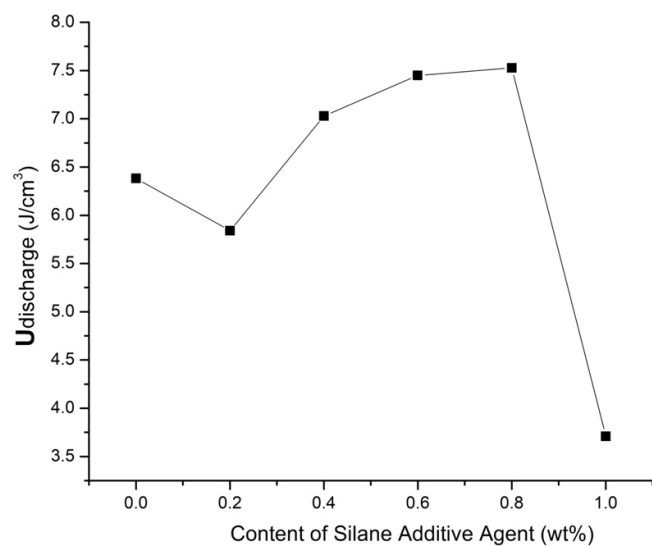


Figure 3-37 Energy density of P(VDF-HFP) thin film with different concentrations of silane for discharging process.

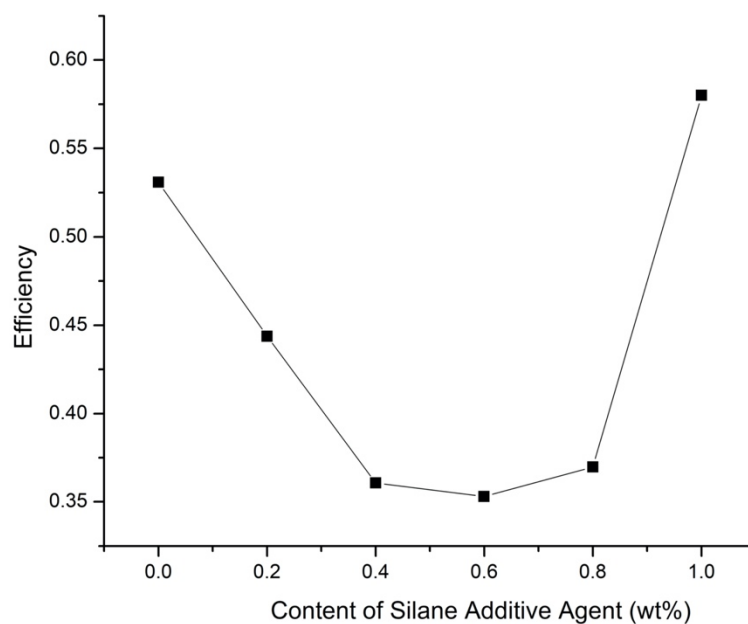


Figure 3-38 Efficiency of P(VDF-HFP) thin film with different concentrations of silane.

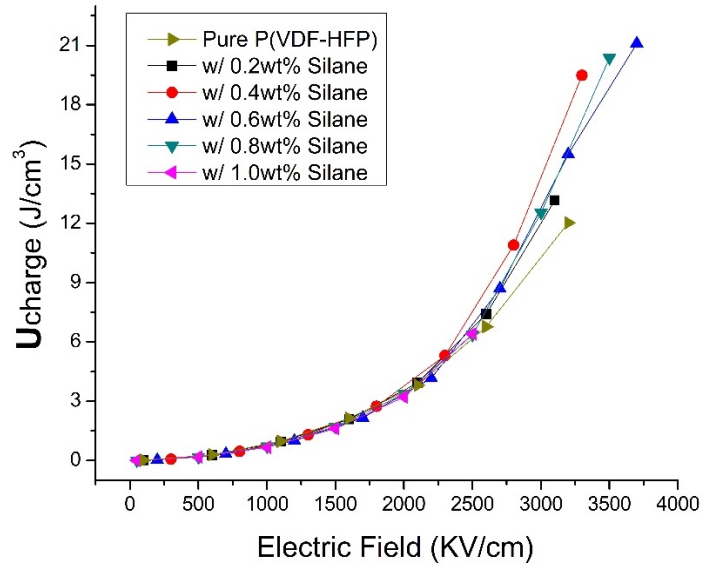


Figure 3-39 Energy density of P(VDF-HFP) thin film with different concentrations of silane for the charging process under different electric fields.

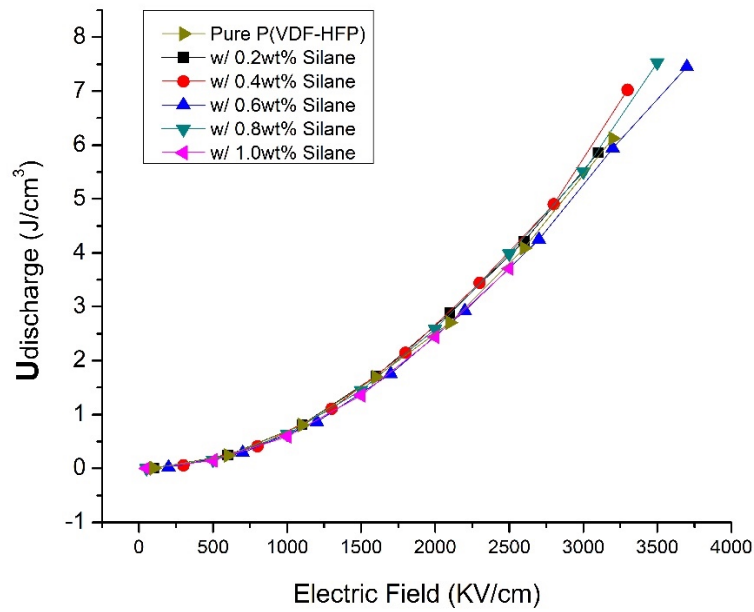


Figure 3-40 Energy density of P(VDF-HFP) thin film with different concentrations of silane for the discharging process under different electric fields.

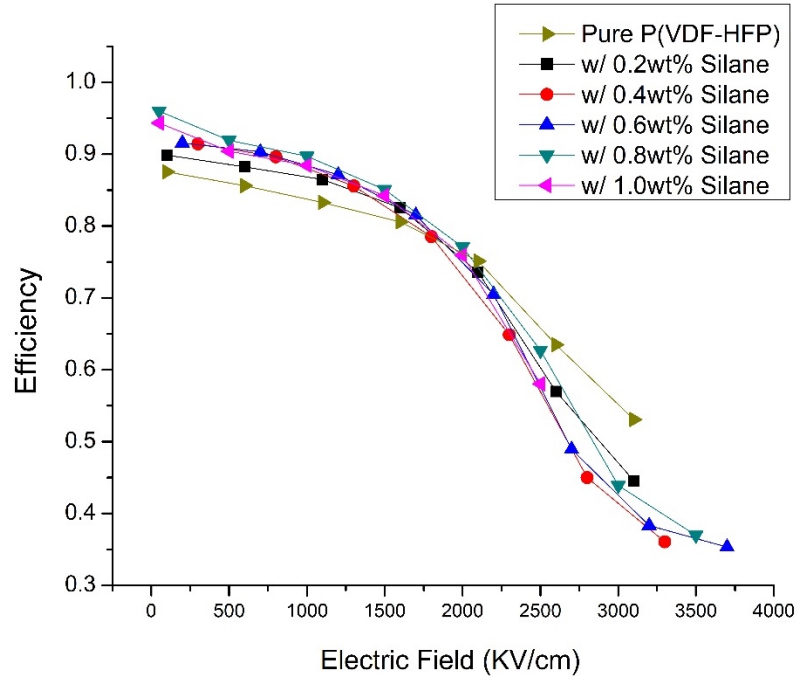


Figure 3-41 Efficiency of P(VDF-HFP) thin film with different concentrations of silane under different electric fields.

3.3.4 Differential Scanning Calorimeter (DSC) test

Figure 3-42~3-43 showed the result of the DSC test for the P(VDF-HFP) thin film with silane from 0wt% to 1.0wt%. All the samples were prepared in the same quench condition, which is 160°C for 15 minutes and immediately put in the ice water. It can be found a second peak existed around 160°C. When compared this result to the previous result, it is related to the dielectric strength; when the intensity of this peak increased, the dielectric strength increased at the same time. That explained this second phase can sustain more electric field than the phase of a wide peak.

Then, **Figure 3-44** showed the enthalpy change based on the DSC result. The enthalpy reached the minimum when adding 0.4wt% of silane. This result indicated that the amount of crystallized polymer reached its minimum. In addition, the sample demonstrated strong

ferroelectric behavior when adding silane above this concentration. Then, the endothermic peak decreased and stabilize when adding silane. Besides, **Figure 3-45~3-47** demonstrated the enthalpy of every peaks and its peak temperature.

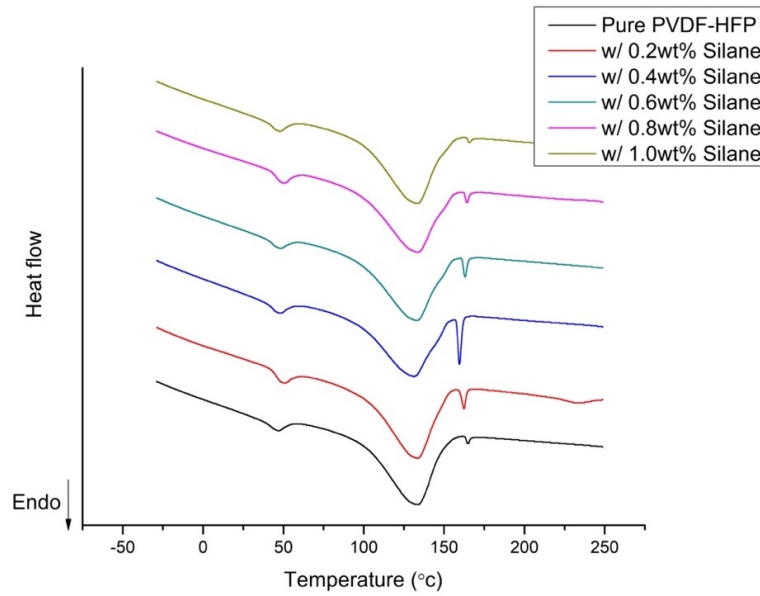


Figure 3-42 The heating process of DSC for P(VDF-HFP) thin film with different concentrations of silane.

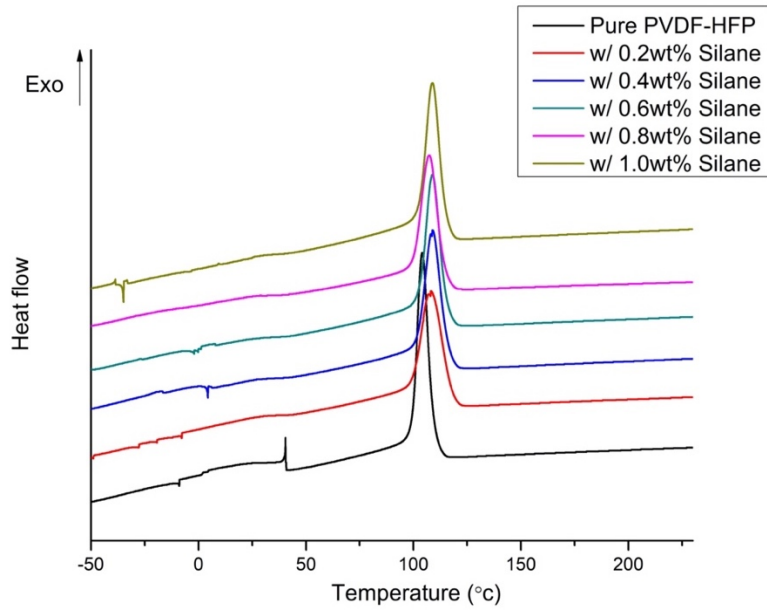


Figure 3-43 The cooling process of DSC for P(VDF-HFP) thin film with different concentrations of silane.

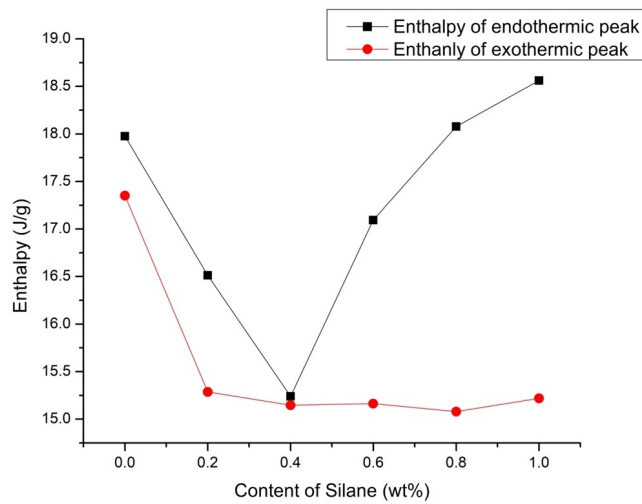


Figure 3-44 Enthalpy of P(VDF-HFP) thin film with different concentrations of silane calculated by DSC result.

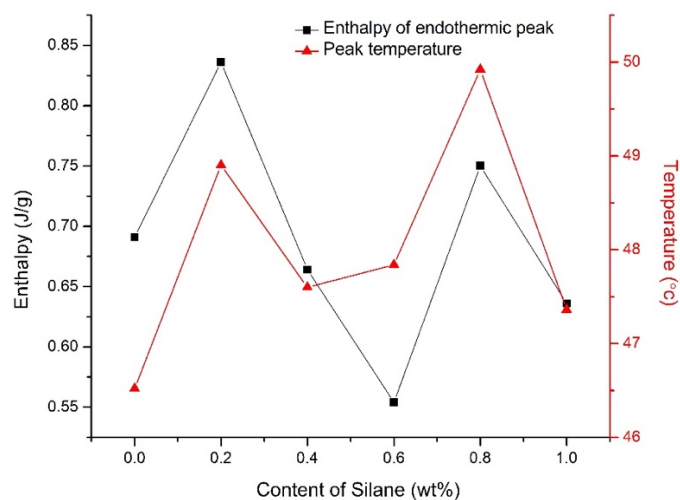


Figure 3-45 Enthalpy and the peak temperature of P(VDF-HFP) thin film with different concentrations of silane at the endothermic peak ($\sim 49^{\circ}\text{C}$) calculated by DSC result.

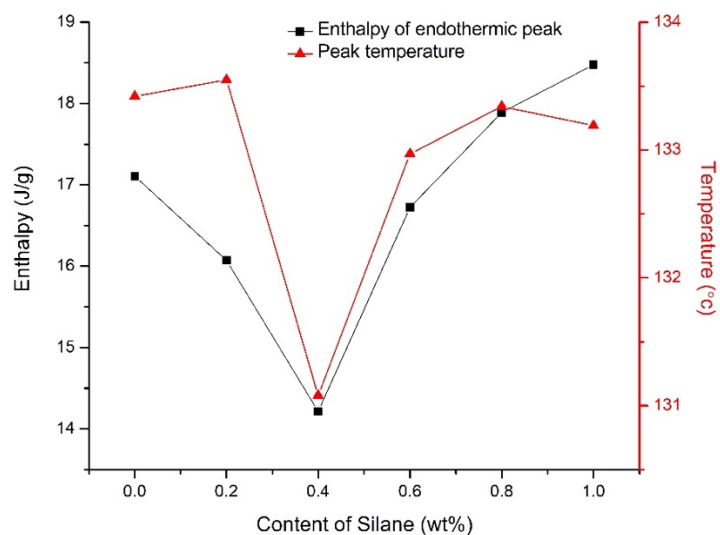


Figure 3-46 Enthalpy and the peak temperature of P(VDF-HFP) thin film with different concentrations of silane at the endothermic peak ($\sim 133^{\circ}\text{C}$) calculated by DSC result.

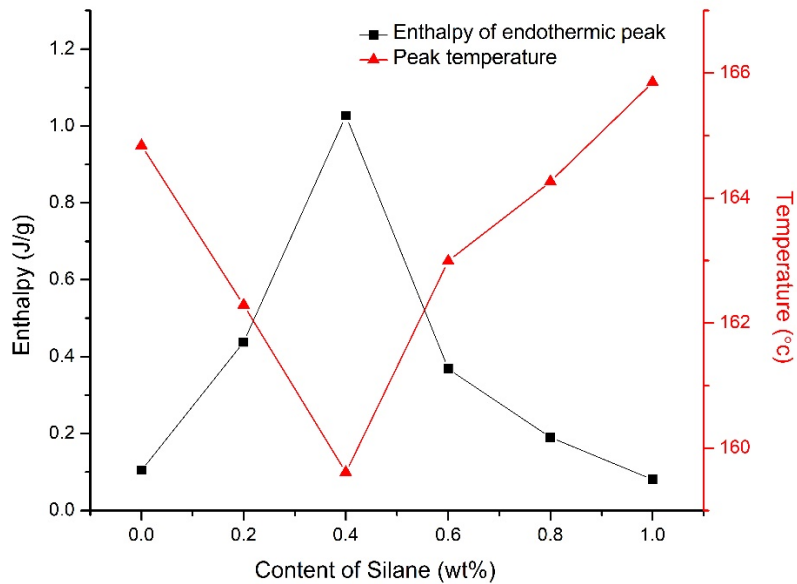


Figure 3-47 Enthalpy and the peak temperature of P(VDF-HFP) thin film with different concentrations of silane at the endothermic peak ($\sim 162^{\circ}\text{C}$) calculated by DSC result.

3.4 Discussion

For the quench experiment of pure P(VDF-HFP) thin film. It exhibited an obvious result that the quench temperature significantly influences the dielectric properties of our P(VDF-HFP) thin film. This phenomenon can be explained by the result of DSC. There existed a second phase for the sample quench at 150°C and 160°C . This second phase can be important evidence for the improvement of permittivity between those two quench temperatures. This second phase probably was the α phase of P(VDF-HFP), based on the results reported in other studies of P(VDF-HFP) **ref 44, 45**. However, if the quench temperature is too high, permittivity went down. In my experiments not reported here, it was found that if applied the quench temperature above 190°C , some visible holes on the thin film were observed. Additionally, the size and number of holes increased with increasing quench temperature. Similar experimental results were also reported in

other studies on the **ref 46**. Those microdefects would make the dielectric properties worse. Therefore, the change of the permittivity can be well explained based on this concept.

Moreover, the dielectric strength decreases with increasing quench temperature. This may also relate to the microdefect. The microdefect results in a low breakdown strength. Therefore, the dielectric strength significantly relates to the number and size of microdefects. This concept can be explained by this phenomenon. Overall, the appropriate quench temperature can get the minimum microdefects and the maximum proportion of the α phase. Therefore, the energy density can reach to the maximum when quenching the pure P(VDF-HFP) thin film at 160°C.

For the P(VDF-HFP) with silane thin film, the permittivity gradually increases initially with increasing silane content; however, when the concentration of silane reached 1.0wt%, the dielectric constant decrease rapidly. This phenomenon can be explained by the free volume theory. The silane molecular would fill up the free space between polymer chains and make the polymer denser and uniform. In the beginning, those free space was occupied by air which has permittivity around 1. Then, when those spaces filled up by the silane, it can improve the dielectric constant and the dielectric breakdown strength of the thin film. However, when the amount of silane exceeds the free space, the dielectric property would become worse because the extra silane can be treated as microdefects.

From the viewpoint of the P-E loop, it can be found that the sample exhibited strong ferroelectricity when the amount of silane over 0.4wt%. It explained that adding silane can increase the ferroelectricity. However, the sample with 1.0wt% silane does not have a ferroelectric phenomenon. This is due to the low dielectric breakdown strength, meaning that the film occurred breakdown before it exhibited the ferroelectric property. Overall, adding silane as a coupling agent to the P(VDF-HFP) thin film can definitely increase the energy density about 20%. However, the efficiency decreased a lot due to the ferroelectric effect.

Chapter 4

Conclusion and Future work

4.1 Conclusion

The P(VDF-HFP) thin film was improved by the thermal treatment and adding silane experiment. The dielectric constant of P(VDF-HFP) thin film with thickness about 12um increased around 9% and energy density increased around 42% after passing two processes, which is helpful for the energy storage. 160°C is the best quench temperature in the heat treatment experiment. From this process, the dielectric constant of pure P(VDF-HFP) thin film can reach 14.3, energy charge density 12.0 J/cm³, energy discharge density 6.4 J/cm³ and dielectric breakdown strength 360 MV/m. Then, 0.8wt% of silane has the best performance for energy storage concern. The dielectric constant of it is 14.6, energy charge density 20.1 J/cm³, energy discharge density 7.5 J/cm³ and dielectric breakdown strength 400 MV/m. Overall, the increment of the dielectric properties and the energy density were basically contributed by the modification of microstructure, containing the different phases of the P(VDF-HFP) and the small molecular. The appropriate temperature can get the phase with better dielectric properties and the lowest defect at the same time. The appropriate amount of silane can fill up the free volume between polymers chains, which can improve the polarization and the dielectric breakdown strength.

4.2 Future work

In general, the dielectric properties of P(VDF-HFP) thin films were examined. However, some assumptions and explanations in this study need to do further analysis using other structure characterization techniques, such as XRD and FTIR. Those two methods can help us to understand the morphology of the sample. In this way, the detail of the composition and can be analyzed. In addition, the temperature dependence of dielectric properties can be also added to this study.

Therefore, it can help us realize the P(VDF-HFP) more comprehensively. Plus, different coupling agents can be analyzed, too. Therefore, it perhaps can fabricate a thin film with higher permittivity and energy density.

In addition, spin coating can be the next approach to reduce the thickness of our sample. From the breakdown theory mentioned in chapter 1, the thinner film can further enhance the dielectric properties. Therefore, the thickness dependence of dielectric properties can be also added to this study. Plus, spin coating can get the films with a different property because of the faster solidification process. The reason for that is the micro-crack would easy to generate during the solution casting process. Those defects negatively influence on the dielectric performance. Therefore, utilizing spin coating to fabricate the thin film may give us more information of the P(VDF-HFP).

Finally, P(VDF-HFP) thin film with a silane experiment showed a very unique result of P-E loop measurement. This result exhibit a strong ferroelectric or antiferroelectric effect. Therefore, it can be a good start point to further analyze the P(VDF-HFP) thin film with silane. Hence, adding silane in different kinds of the polymer can be a good perspective to fortify the effect of silane.

Reference

- [1]. K. C. Kao, Dielectric Phenomena in Solids, Elsevier Academic Press, San Diego, CA 2004.
- [2]. A. V. Hippel, Dielectric Materials and Applications, Technology Press of MIT, Cambridge, Boston 1954.
- [3]. Rao, Y.; Ogitani, S.; Kohl, P.; Wong, C. P. J. Appl. Poly. Sci 2002, 83, 1084-1090.
- [4]. Rao, Y.; Wong, C. P. J. Appl. Poly. Sci 2004, 92, 2228-2231.
- [5]. Zhang, Q. M.; Li, H.; Poh, M.; Xia, F.; Cheng, Z.-Y.; Xu, H.; Huang, C. Nature 2002, 419, (19), 284-287.
- [6]. Newnham, R. E. Ann. Rev. Mat. Sci 1986, 16, 47-68.
- [7]. Dias, C. J.; Das-Gupta, D. K., Ferroelectric Polymer and Ceramic-Polymer Composites. Trans Tech Publications Ltd., Switzerland: 1994.
- [8]. Ieda, M., et al. "Dielectric Breakdown of High Temperature Polymers." 3rd Int. Symp. on High Voltage Eng.. Vol. 21. 1979.
- [9]. Hummel, Rolf E. Electronic properties of materials. Springer Science & Business Media, 2011.
- [10]. Zhang, L. I. N., and Z-Y. Cheng. "Development of polymer-based 0–3 composites with high dielectric constant." Journal of Advanced Dielectrics 1.04 (2011): 389-406.
- [11]. Irodov, Igor' Eugen'evich, Natasha Deineko, and Ram Wadhwa. Basic laws of electromagnetism. Imported Pubn, 1986.
- [12]. Shan, Xiaobing. High dielectric constant 0-3 ceramic-polymer composites. Auburn University, 2009.
- [13]. Zhang, Lin. Fundamental study and development of 0-3 dielectric composites with high dielectric constant. Diss. 2013.
- [14]. Barsoum, M. W., Fundamentals of Ceramics. Institute of Physics Publishing: Bristol and Philadelphia, 1997.
- [15]. Barsoum, Michel, and M. W. Barsoum. *Fundamentals of ceramics*. CRC press, 2002.
- [16]. Barsoum, M. W., Fundamentals of Ceramics. Institute of Physics Publishing: Bristol and Philadelphia, 1997.
- [17]. Wang, Wei. Novel Metal-Polymer Composite with High Percolation Threshold. Diss. 2012.
- [18]. Chen, Lin-Feng, et al. Microwave electronics: measurement and materials characterization. John Wiley & Sons, 2004.

- [19]. Xie, H. K.; Kao, K. C. *IEEE Trans Electr Insul* 1985, EI-20, 293-294.
- [20]. Kittel, C., *Introduction to Solid State Physics*. Wiley: New York, 1988.
- [21]. Mitsui, T., *An introduction to the Physics of Ferroelectrics*. Gordon and Breach Science
- [22]. M. W. Barsoum, *Fundamentals of Ceramics*, Institute of Physics Publishing, Bristol and Philadelphia, 1997.
- [23]. Baojin Chu; Xin Zhou; Kailiang Ren; Bret Neese; Minren Lin; Qing Wang; F. Bauer; Q.M. Zhang. *Science* 2006, 313, (21), 334-336.
- [24]. Arbatti, M. *Development of High-Dielectric-Constant Polymer-Ceramic Composites Based on Calcium Copper Titanate*. Auburn University, Alabama, 2004.
- [25]. Chu, Baojin, et al. "A dielectric polymer with high electric energy density and fast discharge speed." *Science* 313.5785 (2006): 334-336.
- [26]. Branwood, A.; Hurd, J. D.; Tredgold, R. H. *Br.J.Appl.Phys.* 1962, 13, 528.
- [27]. Meng, Qingjie, et al. "Effect of poly (methyl methacrylate) addition on the dielectric and energy storage properties of poly (vinylidene fluoride)." *Journal of applied polymer science* 116.5 (2010): 2674-2684.
- [28]. Zhao, Xiaojia, et al. "Exploring the relationship of dielectric relaxation behavior and discharge efficiency of P (VDF-HFP)/PMMA blends by dielectric spectroscopy." *Materials Research Express* 3.7 (2016): 075304.
- [29]. Gregorio, R., M. Cestari, and F. E. Bernardino. "Dielectric behaviour of thin films of β -PVDF/PZT and β -PVDF/BaTiO₃ composites." *Journal of Materials Science* 31.11 (1996): 2925-2930.
- [30]. Gregorio, R.; Jr., M. C.; Bernardino, F. E. *J. Mater. Sci.* 1996, 31, 2925-2930.
- [31]. Wagner, Karl Willy. "The physical nature of the electrical breakdown of solid dielectrics." *Journal of the American Institute of Electrical Engineers* 41.12 (1922): 1034-1044.
- [32]. Rogowski, W. "Der elektrische Durchschlag von Gasen, festen und flüssigen Isolatoren." *Electrical Engineering (Archiv für Elektrotechnik)* 23.5 (1930): 569-578.
- [33]. Keller, K.J. Formation and annulment of space charges glass and their influence on electric breakdown. *Phys. Rev.* 1952, 86, 804–805.
- [34]. Zheng, F.; Zhang, Y.; Xiao, C. Relationship between breakdown in polymer dielectrics and space charge. *J. Mater. Sci. Eng.* 2006, 24, 316–320.
- [35]. Ieda, Masayuki. "Dielectric breakdown process of polymers." *IEEE Transactions on Electrical Insulation* 3 (1980): 206-224.

- [36]. Fischer, Peter HH, and Kurt W. Nissen. "The short-time electric breakdown behavior of polyethylene." *IEEE Transactions on Electrical Insulation* 2 (1976): 37-40.
- [37]. Whitehead, S. "Dielectric Breakdown of Solids, Chap."
- [38]. Stark, K. H., and C. G. Garton. "Electric strength of irradiated polythene." *Nature* 176.4495 (1955): 1225.
- [39]. Nagao, Masayuki, et al. "Dielectric Breakdown of Ethylene-Vinyl Acetate Composit Polymers in Low-Temperature Region." *The transactions of the Institute of Electrical Engineers of Japan. A* 97.12 (1977): 617-622.
- [40]. Fox Jr, Thomas G., and Paul J. Flory. "Second-order transition temperatures and related properties of polystyrene. I. Influence of molecular weight." *Journal of Applied Physics* 21.6 (1950): 581-591.
- [41]. Nagao, Masayuki, et al. "Dielectric Breakdown of Ethylene-Vinyl Acetate Composit Polymers in Low-Temperature Region." *The transactions of the Institute of Electrical Engineers of Japan. A* 97.12 (1977): 617-622.
- [42]. Miyairi, K., et al. "Dielectric breakdown of polyethylene at low temperature." *J. Inst. Elect. Engrs. of Japan* 91 (1971): 1962-1968.
- [43]. Junjie Li, Qingjie Meng, Wenjing Li and Zhicheng Zhang. "Influence of Crystalline Properties on the Dielectric and Energy Storage Properties of Poly(vinylidene fluoride)" *Journal of Applied Polymer Science*, 122(2011) 1659–1668
- [44]. Liuxia Ruan, Xiannian Yao, et al. "Properties and Applications of the β Phase Poly(vinylidene fluoride)" *Polymers* 2018, 10, 228
- [45]. R.E. Sousa, J. Nunes-Pereira "Microstructural variations of poly(vinylidene fluoride co-hexafluoropropylene) and their influence on the thermal, dielectric and piezoelectric properties" *Polymer Testing* 40 (2014) 245-255.
- [46]. Siva, Divya & Hemalatha, J. "Study on the enhancement of ferroelectric β phase in P(VDF-HFP) films under heating and poling conditions " *European Polymer Journal* 88 (2017) 136–147.